A TIME INTEGRATION PROCEDURE FOR ELASTO-VISCOPLASTIC CONSTITUTIVE EQUATIONS OF THE INTERNAL VARIABLE TYPE

by

MAGIN F. BRICEÑO B.

B.S. Boston University
(1983)

SUBMITED TO THE DEPARTMENT OF MECHANICAL ENGINEERING IN PARTIAL FULFILLMENT OF THE REQUIREMENTS FOR THE DEGREE OF

MASTER OF SCIENCE IN MECHANICAL ENGINEERING

at the

MASSACHUSETTS INSTITUTE OF TECHNOLOGY

January 1985

Signature of Author _____
Department of Mechanical Engineering
January, 1985

Certified by _____
Lallit Anand
Thesis Supervisor

Accepted by _____
Ain A. Sonin
Chairman, Departmental Graduate Committee

A TIME INTEGRATION PROCEDURE FOR ELASTO-VISCOPLASTIC CONSTITUTIVE EQUATIONS OF THE INTERNAL VARIABLE TYPE

by

MAGIN F. BRICEÑO B.

Submitted to the Department of Mechanical Engineering on January 18, 1985, in partial fulfillment of the requirements for the degree of Master of Science in Mechanical Engineering.

ABSTRACT

An implicit, one-step, forward gradient method is developed for the time integration of stiff elasto-viscoplastic equations of the internal variable type. Our method refines and extends the method recently proposed by Pierce, Shih and Needleman [1] in four important respects: (1) It does not use the equivalent plastic strain as an internal state variable. (2) It takes into account any possible change in the "direction" of visco-plastic flow in a time step. (3) It allows for an automatic control of the time step based on certain accuracy considerations. And (4) it is implemented in a state-of-the-art robust, general-purpose, non-linear finite element code ABAQUS [2].

Several representative problems are solved using internal variable constitutive equations for elevated temperature deformation proposed by Anand [3]. Special attention is given to the solution of a creeping thick-walled cylinder under internal pressure and, the upsetting of a cylindrical billet.

Thesis Supervisor: Dr. Lallit Anand
Title: Esther and Harold E. Edgerton
Associate Professor of Mechanical
Engineering

ACKNOWLEDGEMENTS

The author expresess his appreciation to Professor L. Anand. His invaluable guidance and advice were vital to this effort.

I would like to thank my Friend Ed Zywicz for his countless technical contributions and his continuous support and encouragement.

The author wishes to express his appreciation to Professor D. Parks for his interest and constructive observations, and to David Hablanian for his friendship and helpful discussions.

I would like to express my gratitude to FGMA, The Gran Mariscal de Ayacucho Foundation, that gave some of the financial support to make possible this study.

Lastly, and most important, I thank my parents and sister for their unfailing love and moral support.

TABLE OF CONTENTS

LIST OF FIGURES

TITLE PAGE

LIST OF TABLES

Chapter 1

INTRODUCTION

In the past decade or so, a substantial body of work [3-5] on internal variable constitutive equations has developed. The main attributes of this class of constitutive equations are that (a) they do not artificially decompose the inelastic strain increment into a rate idependent "plastic" part and a rate-dependent "creep" part; (b) they do not use any yield conditions or attendant loading/neutral-loading/unloading criteria; and (c) they employ scalar and tensor valued "internal" variables to model the resistance to plastic flow offered by the internal state of the material. Such constitutive equations are numerically very stiff [6], and this has prevented an easy implementation of this class of constitutive equations into general-purpose finite element codes. Recently, Pierce et al [1] have developed an effective one step forward gradient time integration scheme which leads to a tangent stiffness type method for viscoplastic solids. However, the work of Pierce et al [1] is limited in three important respects: (a) it implicitly used the equivalent plastic strain as an

internal variable; (b) it did not account for any possible change in the direction of the plastic flow in a time step; and (c) it did not allow for an automatic control of the time step.

It is the purpose of this thesis to report on our attempts at extending the work of Pierce et al [1] to remedy this differences. We also report on our successful efforts to incorporate such a time integration procedure in a robust, general-purpose, non-linear finite element program ABAQUS.

For simplicity we have limited our attention to internal variable constitutive equations which employ only a single scalar internal variable. In the application of our analysis procedure to specific problems we have used the special functional forms suggested by Anand [5] for the elevated temperature deformation of metallic materials.

1.1 PREVIOUS WORK ON THE AREA

Numerical integration of stiff equations for inelastic behavior has been researched by several investigators [6-8]. Most of the literature deals with methods to produce accurate and stable solutions, regardless of the cost involved during numerical implementation. One early attempt

to treat the numerical analysis of stiff equations was performed by Cyr et al [7]. They performed a finite element solution of elastic-plastic-creep problems using axisymmetric and plane stress conditions. This work concluded that one of the major problems was the choice of the right time increment size which largely depends on the stress level and the change of the creep strain rate. The method they proposed could easily be extended for other plastic and creep flow laws.

Some of these methods have been reviewed by Willam [8]. Based upon stability and accuracy criteria, he compared each of the most used methods to solve stiff equations. Implicit and explicit methods are the two main groups of numerical integration methods, as presented by Willam, and the main disadvantages of each group are discussed. The author concludes that the use of implicit methods ,such as the Euler backwards method, are to be prefered if the solution's stability is the major concern. This is so, because of the unconditional stability property pertaining to implicit procedures. The main disadvantage in using implicit integration, as concluded by Willam, is that very expensive interative techniques are required to reach approximate solutions, thus reducing the solution procedure's effectiveness.

A good review of numerical integration methods of

unified plasticity-creep formulations is presented by Krieg [6]. He describes some of the most recent constitutive models for plasticity-creep phenomena, using a generalized framework based on a unified inelastic strain. As Kreig observes, all these models are well behaved in some regions and very "stiff" in others. The use of conventional integration methods with these equations becomes totally inadequate [6]. He suggests two integration methods that could be used to solve stiff equations: (1) an Euler forward predictor method with a trapezoidal corrector and (2) a backward Euler method with a Picard interation. Kreig, based on theoretical analysis only, concludes that method (2) will be best suited to solve these models, given its unconditional stability property. No finite element form was presented in his paper.

Shih, Delorenzi and Miller [9] present a study of several integration techniques to solve time dependent constitutive equations. They tested explicit models, such as Euler forward integration, as well as implicit techniques such an implicit trapezoidal rule that uses a strongly convergent Newton's method. The investigators tested these models with the help of a finite element program by solving a thick walled tube under mechanical and thermal loadings. They found that if the implicit method were modified by introducing the Taylor's expansion of the main variables, thus removing the method's implicitness [9], they could

obtain accurate and stable solutions with almost 1/5 of the time that the Newton's method used.

Using a different method, Pierce et al. [1] analyzed the solution of several rate dependent equations, such as creep problems. The method they used is called the Ø-method, proposed by [7] and extended by [10]. It uses two parameters: the time step, dt, and the Ø-parameter, which handles the method's degree of implicitness. They solved typical problems with different choices of Ø and dt looking for stability and accuracy. It is stated that since the plastic strain changes with each time step increment, additional restrictions on the choice of dt are imposed. Thus, if the plastic strain undergoes large changes from one step to the other, smaller dt's should be used, and larger dt's should be used for the opposite case. These findings imply that only in certain parts of the test should small dt's be used to assure stability, but larger dt's can be used for the remainder of the test.In this way the effectiveness of the solution could be greatly improved. Pierce et al made these time step changes manually. This means they knew beforehand when the small time steps should be used, a case that only occurs in a few problems. To overcome this problem, some kind of automatic time step control is desirable.

1.2 SCOPE OF THIS THESIS

The purpose of this thesis is to develop a numerical integration procedure based on the Ø-method and which uses an automatic time step control strategy such an approach can be used to solve hot working equations.

Towards this goal, a set of analytical models as well as some experimental tests were implemented. Chapter 2 describes in detail the set of constitutive equations that will be used in this research , as well as the general notation followed. Chapter 3, contains a general study of the stability characteristics of the Ø-method and the criterions for stability are presented. Also, a discussion of stiffness of inelastic equations is presented. The solution procedure to solve one dimensional problems is shown in Chapter 4. A set of uniaxial loading cases are modeled to show the effectiveness of the model presented.Chapter 5 extends the procedure to a fully 3-D case and examples are included. A thick wall cylinder experiment is explained in Chapter 6 and compared with the finite element solution results. FORTRAN codes used in this research are presented in the appendices.

Chapter 2

CONSTITUTIVE EQUATIONS FOR HOT WORKING PROCESSES

2.1 INTRODUCTION

The constitutive equations used in this research are the equations for the analysis of rate dependent deformations of metals at high temperatures, developed by Anand [5]. The following chapter outlines these hot working equations in both one and three dimensional formats. A full description of the variable notation used is summarized.

2.2 HOT WORKING EQUATIONS FOR MULTIAXIAL PROBLEMS

First, we introduce the notation that will be followed in this section:

- $\underline{F}$ denotes the deformation gradient
- $\underline{D} := \text{sym}\,(\dot{\underline{F}}\,\underline{F}^{-1})$ is the stretching tensor
- $\underline{W} := \text{skw}\,(\dot{\underline{F}}\,\underline{F}^{-1})$ is the spin tensor

- $\underline{T}$ is the Cauchy stress tensor

- $\tilde{\underline{T}} := (\det\underline{F})\underline{T}$ is the Kirchhoff stress tensor

This notation will be used to describe the constitutive equations for isotropic thermo-elasto-viscoplasticity with isotropic hardening proposed by Anand [11].

2.2.1 The stress-strain temperature relation

Let us assume that $\underline{D}$, the total stretching, could be written as the sum of $\underline{D}^e$, the elastic stretching, and $\underline{D}^p$, the plastic stretching

$$\underline{D} = \underline{D}^e + \underline{D}^p \qquad 2.2.1$$

Then, the Jaumann derivative of the Kirchhoff stress can be represented by

$$\overset{\nabla}{\tilde{\underline{T}}} = \underline{L}\,(\underline{D} - \underline{D}^p) - 3\kappa\alpha\dot{\theta}\underline{1} \qquad 2.2.2$$

Here

$$\overset{\nabla}{\tilde{\underline{T}}} := \dot{\tilde{\underline{T}}} - \underline{W}\,\tilde{\underline{T}} + \tilde{\underline{T}}\,\underline{W} \qquad 2.2.3$$

where $\dot{\theta}$ is the temperature's rate of change, $k(\theta)$ is the bulk modulus, and $\alpha(\theta)$ corresponds to the coefficient of thermal expansion. The elasticity tensor, $\underline{L}$, is represented by

$$\underline{L} = 2\mu\underline{I} + (\kappa - (\tfrac{2}{3})\mu)\,\underline{1}\otimes\underline{1} \qquad 2.2.4$$

where $\mu(\theta)$ is the shear modulus and $\underline{I}$ is the identity tensor.

2.2.2 the flow rule

The plastic stretching can be expressed by

$$\underline{D}^p = \dot{\gamma}^p \left(\frac{\underline{\tilde{T}}'}{2\tilde{\tau}} \right) \qquad 2.2.5$$

where $\dot{\gamma}^p$ is the equivalent plastic strain rate, $\underline{\tilde{T}}'$ is stress deviator, and $\tilde{\tau}$ is the equivalent shear stress, given by

$$\tilde{\tau} = \left| \left[\left(\tfrac{1}{2}\right) \text{trace}\left(\underline{T}'^2 \right) \right]^{\frac{1}{2}} \right| \quad . \qquad 2.2.6$$

Equation 2.2.5 constitutes the flow rule to be used.

If we define an equivalent tensile stress such that

$$\tilde{\sigma} = \left[(3)^{\frac{1}{2}} \right] \tilde{\tau} \qquad 2.2.7$$

and, an equivalent plastic tensile strain, $\dot{\epsilon}^p$ represented by

$$\dot{\epsilon}^p = \frac{\dot{\gamma}^p}{(3)^{\frac{1}{2}}} \qquad 2.2.8$$

we could replace eq. 2.2.5 with

$$\underline{D}^p = (3/2)\, \dot{\epsilon}^p \left(\frac{\underline{\tilde{T}}'}{\tilde{\sigma}} \right) \quad . \qquad 2.2.9$$

2.2.3 The evolution equation

The equivalent plastic strain rate, $\dot{\epsilon}^p$, used in eq.2.2.8 is assumed to be a function of stress, temperature, and a set of internal variables, α_n. The equivalent plastic strain rate can be written as

$$\dot{\epsilon}^p = f\left(\tilde{\sigma}, \theta, \alpha_n \right) \qquad 2.2.10$$

where **f** is the function form of $\dot{\bar{\epsilon}}^p$. Here, the set of variables α_n consist of several values which represent the material's internal behavior. As an approximation and to ease the numerical analysis, it is assumed that α_n is composed of a single variable **s**, which represents an intrinsic deformation resistance to plastic flow offered by the internal defect and microstructural state of the material element [5]. Thus, the evolution of the variable **s** can be assumed to be a function of stress, temperature, and **s**, such that

$$s = h(\bar{\sigma}, \theta, s) . \qquad 2.2.11$$

s could be assumed to be formed by two different functions since it is assumed that **s** can change even if $\dot{\bar{\epsilon}}^p = 0$. Thus,

$$\dot{s} = h(\bar{\sigma}, \theta, s) \dot{\bar{\epsilon}}^p - r(\theta, s) \qquad 2.2.12$$

where **h** represents the strain hardening rate and **r** represents the rate of static recovery of **s**. Furthermore, we can also represent the strain hardening rate as two components, h_1 and h_2 which represent strain hardening and strain softening respectively. Thus

$$h(\bar{\sigma}, \theta, s) = h_1(\bar{\sigma}, \theta, s) - h_2(\bar{\sigma}, \theta, s) \qquad 2.2.13$$

So far, we have presented a general format for the development of elasto-viscoplastic equations with isotropic hardening. We now proceed to present Anand's [10] equations, which are special cases of equations 2.2.10 to 2.2.11. The equivalent plastic strain rate, $\dot{\bar{\epsilon}}^p$, is assumed

to be

$$f(\tilde{\sigma},s,\vartheta) = A\left[\exp\left(\frac{-Q}{R\vartheta}\right)\right]\left(\tilde{\sigma}/s\right)^{1/m} \quad , \qquad 2.2.14$$

where **R** is the universal gas constant, **Q** represents the material's activation energy, **m** is the strain rate sensitivity, and **A** is a nonzero positive parameter. The variable **m** is assumed to be a function of temperature only.

The evolution of the internal variable **s**, from eq.2.2.11 can be written as

$$\dot{s} = h_0\left(1 - \frac{s}{s^*}\right)\dot{\bar{\varepsilon}}^p - r \qquad 2.2.15$$

where

$$s^* = \tilde{s}\left[\frac{\left|\dot{\bar{\varepsilon}}^p\right|}{A}\exp\left(\frac{Q}{R\vartheta}\right)\right]^n \qquad 2.2.16$$

Where h_0 and **s** are material quantities.

The degree of agreement between the theory proposed by Anand and experimental stress-strain data for an Fe-0.05 weight percent steel at elevated temperatures as shown in his figures 1 and 2 of his 1982 paper are reasonable. It is important to note that no equations for the static restoration function **r** were proposed by Anand [5] because of lack of adequate data. However, Anand [11] has recently suggested that the following empirical form of the static restoration function should be

$$r = \mu A B \left[\exp\left(\frac{-Q}{R\vartheta}\right) \right] \left\langle \frac{s}{s_a} - 1 \right\rangle^p \qquad 2.2.17$$

where **B** and **p** are additional material constants, s_a is the fully annealed value of **s** and $\langle x \rangle$ is the singularity map defined by

$$\langle X \rangle = \begin{cases} X & \text{if } X > 0 \\ 0 & \text{if } X < 0 \end{cases} . \qquad 2.2.18$$

For purposes of numerical experimentation we adopt this form here.

In addition to the equations given above, we will assume that the temperature ϑ evolves according to

$$\dot{\vartheta} = \frac{\omega}{\rho C} \underline{\underline{T}} \cdot \underline{\underline{D}}^p \qquad 2.2.19$$

Where ρ is the mass density and **C** the specific heat. This evolution equation for ϑ assumes no thermal conduction. With $0.85 < w < 1$ may suitable represent the temperature change under very rapid loadings. Of course, to calculate $\dot{\vartheta}$, in general one has to solve the coupled thermo mechanical problem.

2.3 CONSTITUTIVE EQUATIONS FOR UNIAXIAL PROBLEMS

We will first discuss our time integration procedure

for one-dimensional problems. For such situations the constitutive equations analogous to those of the previous section are: (a) the rate stress temperature relation

$$\dot{\sigma} = E (\dot{\epsilon} - \dot{\epsilon}^{p}) - 3\kappa\sigma\dot{\vartheta} \qquad 2.3.1$$

(b) the flow rule

$$\dot{\epsilon}^{p} = A \left[\exp \left(\frac{-Q}{R\vartheta} \right) \right] \left(\sigma / s \right)^{1/m} \mathrm{sign}(\sigma) \qquad 2.3.2$$

(c) the evolution equation for s is

$$\dot{s} = h_0 \left(1 - \frac{s}{s^{*}} \right) | \dot{\epsilon}^{p} | - A B E \left\{ \exp \left(\frac{-Q}{R\vartheta} \right) \left\langle \frac{s}{s_a} - 1 \right\rangle^{p} \right\} \qquad 2.3.3$$

where

$$s^{*} = \tilde{s} \left(\frac{| \dot{\epsilon}^{p} |}{A} \exp \left(\frac{Q}{R\vartheta} \right)^{n} \right) \qquad 2.3.4$$

and (d) the evolution for ϑ under the assumptions of no thermal conduction is

$$\dot{\vartheta} = \left(\frac{\omega}{\rho C} \right) | \sigma | | \dot{\epsilon}^{p} | \qquad 2.3.5$$

Chapter 3

NUMERICAL INTEGRATION PROCEDURE

3.1 INTRODUCTION

The following chapter presents the numerical procedure that we have used throughout our work. Stability analysis,corresponding to the numerical scheme, is also shown. The stiffness term is defined and a justification for the usefulness of the integration method to solve stiff equations is given.

3.2 NUMERICAL INTEGRATION SCHEME

With the plastic strain law expressed in eq. 2.2.14 it is possible to find the solution of ϵ^p_{n+1} at a future time $t=t^{n+1}$ if we know the value of ϵ^p at time $t=t^n$ using

$$\epsilon^p_{n+1} = \epsilon^p_n + \Delta\epsilon^p_n \qquad 3.2.1$$

where the increment $d\epsilon_n$ (we will use d for Δ for the rest of this paper), the plastic strain increment, is defined by

$$\Delta\epsilon^{p}_{n} = \Delta t_{n} [(1 - \phi) f_{n} + \phi f_{n+1}] \qquad 3.2.2$$

where f represents the function of the plastic strain rate, and the parameter Ø has the following possible and meaningful values

$$0 \leq \phi \leq 1 \qquad 3.2.3$$

This time integration procedure is called the Ø-method and it is classified as a linear, one step scheme of order one [12].

By setting Ø=0, we obtain the Euler forward integration scheme, which is also referred as a fully explicit method since the plastic strain increment is completely determined by "explicit" conditions existing at t_n [13]. On the other hand, if Ø=1, the method gives a fully explicit (or backward difference) method, with the plastic strain increment determined from "implicit" strain rates corresponding to the end of the time interval. In general, for any value of Ø>0, there is a certain degree of implicitness introduced in the method.

It can be shown [14] that the time integration scheme presented by eq. 3.2.2 is unconditionally stable for values of Ø≥0.5. This implies that the method is stable for any choice of dt, but it does not guarantee the accuracy of the solution. For this specific case, Ø≥0.5, the method is considered an A-stable method of integration [12]. For the

case of $\emptyset<0.5$ the integration process is only conditionally stable and the numerical time integration can only be stable for values of dt_n less than some critical value, dt_{crt}. This critical value can be shown [1] to be about 10% of the time to reach yield strain, given a test strain rate. Thus, using the equations of chapter 2, we can estimate this value to be

$$\Delta t_{crt} = 0.1 \frac{s_0}{E \dot{\epsilon}} \qquad 3.2.4$$

for the case of Von Mises material, under a tenion test. Here, s_o is the initial value of s, E is the elasticity modulus and $\dot{\epsilon}$ represents the test strain rate.

3.3 STIFFNESS

The problem of stiffness of nonlinear differential equations has been known for some time. But, recently with the availability of high speed computational methods and systems, the problem has captured the attention of many researchers around the field of engineering . The definition of the problem is as follows: given a set of uncoupled differential equations, is said to be stiff if

$$| Re(\lambda_{max}) | >> | Re (\lambda_{min}) | \qquad 3.4.1$$

where the eigenvalues are those of the Jacobian matrix, $\underline{J}$ [9]. This means, that having eigenvalues too far into the

left side of the complex plane will require very small values of **dt** if we use $\emptyset<1/2$. The use of small **dt's** makes the whole procedure very expensive as a result of too many steps required to integrate over a long range of **t**. We can solve this problem by using any A-stable method to integrate the stiff equations , since the **dt** is not bound by any stability condition. The only remaining consideration would be the one related to the choice of **dt** to obtain accurate solution. This suggestion was first made by Dahlquist theorems for stiff equations [12].

It follows from the same Dahlquist theorems that the value of $\emptyset$ which yields the smallest error constants is $\emptyset=1/2$. So the closer we get to $\emptyset=1$, the bigger error we get in approximating the exact solution, but, also a better stability response is obtained. Then, since there is a trade off between stability response and accuracy, the size of $\emptyset$ should be picked taking into account this considerations.

We can now check if the equations presented in chapter 2 are stiff or not. One way to find out is to compute for the Jacobian's eigenvalues and then use eq. 3.4.1 to check for stiffness. However, in most cases involving stiff equations, finding the eigenvalues of $\underline{J}$ is not an easy task, if possible at all. Therefore, we must use a different approach based in the observation of the dependent

variables' evolution . Thus, recalling the set of constitutive equations, it can be appreciated that the stiffness arises from two sources

- The plastic strain rate is strongly dependent on the stress and the internal variable **s**, which means that small changes on σ and **s** causes large changes on $\dot{\epsilon}^p$.

- The evolution of **s** depends on the strain hardening rate and recovery rate. When **s** approaches steady state, $\dot{s}$ is given by a difference of two almost equal quantities, any small change in $\dot{\epsilon}^p$,**h** and **r** would cause large changes in **s** [9].

The integration time step, dt, depends on the magnitude of the variations of **f**,**h** and **r** with respect to σ and **s** (similar as to computing the Jacobian). Thus, if these changes are very large (big eigenvalues), smaller **dt's** will be required, confirming the stiff properties of the equations .

Chapter 4

NUMERICAL SIMULATION OF UNIAXIAL PROBLEMS

4.1 INTRODUCTION

Having defined the specific form of the numerical procedure used in this research, it remains to show how this method of integration, combined with some form of automatic time step control yet to be defined, can be successfully applied to solve problems using the equations for hot working processes presented in Chapter 2.

A series of numerical simulations have been performed to model simple problems in both one and three dimensional cases. These simulations were done using a VAX 11-780 computer, and, the more complicated problems involving 3-dimensional components, were implemented with the help of the finite element program ABAQUS, developed by Hibbit et al [2].

In the following chapter, one dimensional simulations of simple problems are presented. Special tests such as creep and cyclic loadings are emphasized.

4.2 INCREMENTAL FORM OF THE ELASTO-VISCOPLASTIC EQUATIONS

Using eq's 3.2.1 and 3.3.2 we can find the incremental forms of the stress, temperature, internal variable **s**, and the strain . The appropriate values of the variables in question, at a future point in time $t=t_{n+1}$, are given by

$$\sigma_{n+1} = \sigma_n + \Delta\sigma_n \qquad 4.2.1$$

$$\epsilon^p_{n+1} = \epsilon^p_n + \Delta\epsilon^p_n \qquad 4.2.2$$

$$s_{n+1} = s_n + \Delta s_n \qquad 4.2.3$$

$$\vartheta_{n+1} = \vartheta_n + \Delta\vartheta_n \qquad 4.2.4$$

By using the Ø-method, eq.3.2.2, we can find the increments in the above equations. After some algebraic manipulation, it can be shown that eq.'s 4.2.1 and 4.2.4 can be written as functions of dS_n and $d\epsilon^p_n$ only.This implies that it is only necessary to find these two incremental values. We can find the increment in the plastic strain $d\epsilon^p$ using Eq.3.2.2 . This increment is

$$\Delta\epsilon^p_n = \Delta t_n [\, \dot{\epsilon}^p_n + \phi(\dot{\epsilon}^p_{n+1} - \dot{\epsilon}^p_n) \,] \qquad 4.2.5$$

Here, the value of $\dot{\epsilon}_{n+1}$ is unknown, and so, it must be expressed using it's corresponding Taylor's expansion about t_n [1]. Taking $\dot{\epsilon}^p_{n+1}$ as a first order Taylor's expansion, we find that the approximation of $d\epsilon^p$ is

$$\Delta\epsilon^p_n = F_n \Delta t_n \qquad 4.2.6$$

where

$$F_n = \frac{\dot{\epsilon}^p_n}{1 + U_n} \qquad 4.2.7$$

Here, the value of U_n is given by

$$U_n = \phi \Delta t_n C_n \left[E + \left(\beta_n - \frac{G_n}{D_n} \right) \frac{\omega}{\rho C} \sigma - I_n \frac{H_n}{D_n} \right] \qquad 4.2.8$$

where

$$G_n = \partial \dot{\epsilon}^p_n / \partial \theta_n \qquad D_n = \partial \dot{\epsilon}^p_n / \partial \sigma_n \qquad I_n = \partial \dot{\epsilon}^p_n / \partial s_n \qquad 4.2.9$$

Using eq. 3.2.2, the increment of the internal variable **S**, dS_n is expressed as

$$\Delta s_n = \Delta t_n \left[\dot{s}_n + \phi \left(\dot{s}_{n+1} - \dot{s}_n \right) \right] \qquad 4.2.10$$

The result of the corresponding Taylor's expansion, substituted into eq. 4.2.10 and after neglecting all terms of order dt^2 or higher, can be reduced to

$$\Delta s_n = H_n \Delta \epsilon^p_n - \Delta R_n \qquad 4.2.11$$

where

$$H_n = \frac{h_n}{1 + P_n} \qquad 4.2.12$$

and

$$\Delta R_n = \frac{r_n \Delta t_n}{1 + P_n} \qquad 4.2.13$$

Here, the value of P_n is

$$P_n = - \phi \Delta t_n \left[C_n \dot{\epsilon}^p_n + I_n h_n - K_n \right] \qquad 4.2.14$$

where

$$K_n = \partial r_n / \partial s_n \qquad C_n = \partial h_n / \partial s_n \qquad 4.2.15$$

Using eq. 4.2.6 for the increment of the plastic strain, we can write the corresponding temperature's increment. This increment is

$$\Delta\vartheta_n = \frac{\omega}{\rho C} |\sigma||\Delta\epsilon^p{}_n| \qquad 4.2.16$$

Now, using the above equation and eq. 4.2.6, we can write the stress increment used in eq. 4.2.1 . This is

$$\Delta\sigma_n = E \{ \Delta\epsilon_n - \epsilon^p{}_n \} - \beta_n \Delta\theta_n \qquad 4.2.17$$

Also the increment on the total strain becomes

$$\Delta\epsilon_n = \dot{\epsilon}\, \Delta t_n \qquad 4.2.18$$

Then, using the increments represented by eq.'s 4.2.6, 4.2.11, 4.2.15, and 4.2.16 we can substitute back into eq.'s 4.2.1 to 4.2.4 and find the values of σ, S, ϵ and Θ at time $t=t_{n+1}$.

The appropriate choice of the time step is done by means of an automatic time step control algorithm, which is based on the stability conditions presented in Chapter 3.

4.3 AUTOMATIC TIME STEP CONTROL ALGORITHM

As it was explained in Chapter 3, the use of the Ø-method to integrate rate dependent equations requires a

careful choice of the time step to be used at each increment, based on certain considerations related to stability and accuracy. However, it has been shown by Pierce et al [1] that we can choose different time steps during the integration, instead of a fixed time step for the whole test region. This conclusion is made after observing the behavior of the plastic strain rate, during the period of any particular test. The plastic strain rate can change dramatically in certain regions, but it could also remain almost constant for other regions of the same test. For example, let us consider a simple tension test of a material which exhibits plastic behavior. It is known that the plastic strain rate corresponding to the knee area undergoes great changes in size, but, on the other hand in the steady state stress region, the plastic strain rate remains almost constant.

Based on this particular behavior of the plastic strain, we can infer that if the plastic strain rate changes considerably, larger changes are to be expected for some of the other variables in the material equations [9]. In such a case the time steps required to integrate this region need to be small, due to the increased stiffness of the equations. On the other hand, if the plastic strain rate remains almost constant, it will be unnecessary to use small time steps since the changes in the variables of the equations are not too large.

Having these facts in mind, we have designed an automatic time step control algorithm which will use the maximum time step possible in every increment of the integration. This means, that it will use small time steps in areas of vastly changing plastic strain rates, and bigger time steps for areas of steady plastic strain rates. In this way, the amount of steps required to integrate the constitutive equations could be reduced by some amount, without compromising the solution's accuracy. Based on this criteria we have defined an error parameter which defines the maximum allowable increment of the plastic strains, which will be compared against the difference of plastic strains at two consecutive increments. The result of such a comparison will tell us if the size of the time step was the appropriate one for the increment. This error parameter has been called **CETOL** and is defined as

$$CETOL = \delta \frac{s_0}{E} \qquad 4.3.1$$

where δ which controls the accuracy of the integration. This **CETOL** value corresponds to δ times the yield strain of the material. A value of 10^{-2} to 10^{-3} for δ has been found to yield accurate solutions for most of the cases treated during this investigation.

Once **CETOL** has been defined, the algorithm checks **XMDPSI**, the maximum difference of plastic strains corresponding to the present increment. **XMDPSI** is expressed

as

$$XMDPSI = \Delta t_n \left(\dot{\epsilon}^p_{n+1} - \dot{\epsilon}^p_n \right) \qquad 4.3.2$$

After this calculation is performed, the algorithm calculates **RI**, the ratio of **XMDPSI** and **CETOL**, which is represented by

$$RI = \frac{XMDPSI}{CETOL} \qquad 4.3.3$$

Then, if the size of **RI**<1, the value of dt_n is accepted as the appropriate one and the increments of eq.'s 4.2.1 to 4.2.4 are computed. On the other hand if **RI**>1, the actual time step is rejected and it is replaced by 0.85/**RI** times the rejected time step. Then, **XMDPSI** is recomputed using this new time step step. The process is repeated until **RI**<1.

Once the incremental values have been computed, the algorithm proceeds to determine the first trial value of the time step that will be used at the next increment. The next time step, dt_{n+1}, is suggested as a multiple of the presently accepted time step, dt_n, based on the size of **RI**. The value of the next time step is equal to

- if $0.8<RI\leq 1.0$ then $dt_{n+1}=dt_n$
- if $0.7<RI\leq 0.8$ then $dt_{n+1}=1.1dt_n$
- if $0.4<RI\leq 0.7$ then $dt_{n+1}=1.25dt_n$
- if $0.4\geq RI$ then $dt_{n+1}=1.5dt_n$

Also, inside the algorithm there are procedures which will limit the actual sizes of dt_n to fall within a minimum and a maximum time steps. These maximum and minimum values are user supplied.

We could have used another measure for the time step control, other than **XMDPSI**. As an example, we could have used the measure called **XMDIVSI**, the maximum difference of the internal variable **s** increment, and have it compared to a tolerance similar to **CETOL**. However, from the tests performed in this research, we have found that **XMDPSI** represents the most critical measure which changes by a bigger amount than **XMDIVSI**. For this reason, we employ **XMDPSI**.

Using the Ø-method in conjunction with the automatic time step control outlined in this chapter, we have been able to increase the effectiveness of the numerical integration of rate dependent equations within acceptable accuracy values.

4.4 SIMULATION OF UNIAXIAL PROBLEMS USING STEEL

A series of numerical exercises have been made using the material parameters of Fe-0.05 weight percent Carbon steel, which values are shown in table 4.4.1. These tests

TEMPERATURE $\theta = 1323^{o}K$

VARIABLE	VALUE	UNITS
n	0.03	---
m	0.147	---
A	1.0×10^{-11}	1/sec
Q	2.7×10^{-2}	Joule
h_o	1329.22	N MPa
S	147.06	MPa
R	8.31×10^{-3}	Joule/^{o}K
C	0.6482	Joule/^{o}K gm
E	4.21×10^{3}	MPa
α	22×10^{-6}	1/^{o}K
ρ	7.268	gm/cm^3
ν	0.370	----

Strain rate, 1/sec	S_o, MPa
2.3×10^{-2}	47.11
2.4×10^{-3}	51.81
1.4×10^{-4}	48.25

TABLE 4.3.1 MATERIAL PROPERTIES OF Fe-0.05 WEIGHT PERCENT CARBON STEEL

were done to show the effectiveness of the automatic time step control mechanism to integrate simple, one dimensional problems, where there is only one component of strain and one of stress, both in the same direction.

The specific parameters that were used in the numerical method are

$$\phi = 0.75$$
$$\delta = 10^{-3} \qquad 4.4.1$$

The minimum time step allowed, based upon equation 3.2.3, is

$$\Delta t_0 = 0.01 \frac{s_0}{E \dot{\epsilon}} \qquad 4.4.2$$

where $\dot{\epsilon}$ is the test's strain rate. These parameters were chosen based upon several parametric studies done which incorporated the integration method proposed. They represent an acceptable combination of accuracy and stability.

The first series of tests show comparisons made between the method proposed in this research and the Euler forward method using a fixed time step incrementation of $5dt_o$, as defined by eq. 3.2.3. The test consisted of a simple tension test at a constant strain rate $\dot{\epsilon}$, where no recovery effects and isothermal conditions where used; that is r=0 and w=0, respectively. Plots made of the results for both tests are shown in figure 4.4.1. As it can be seen, both tests show very similar results, but, as each data mark

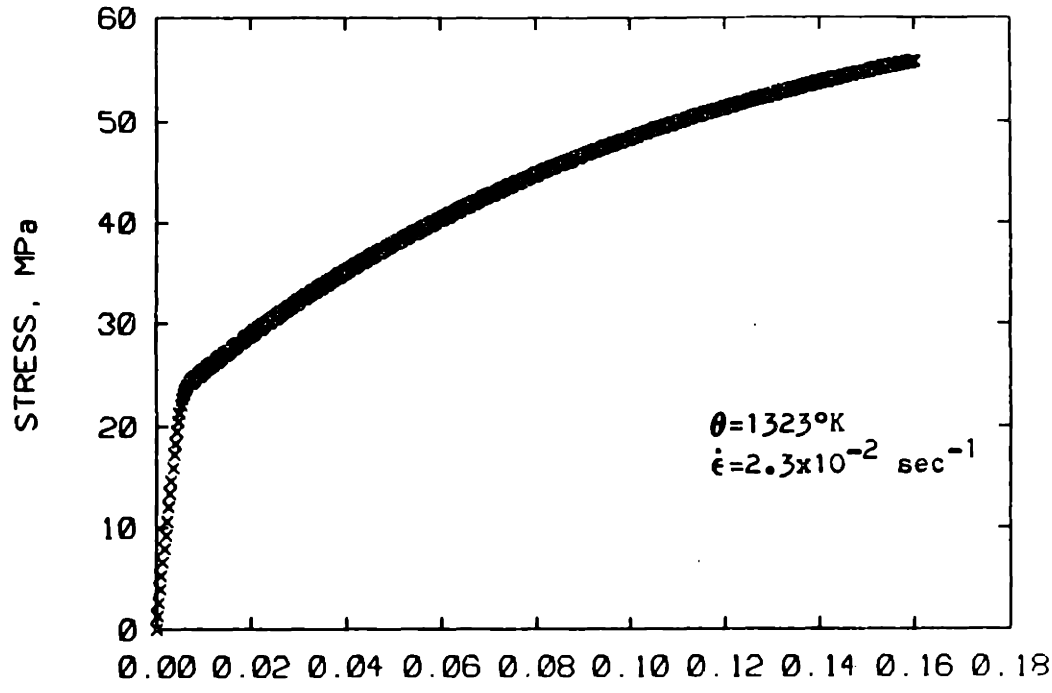

EULER METHOD

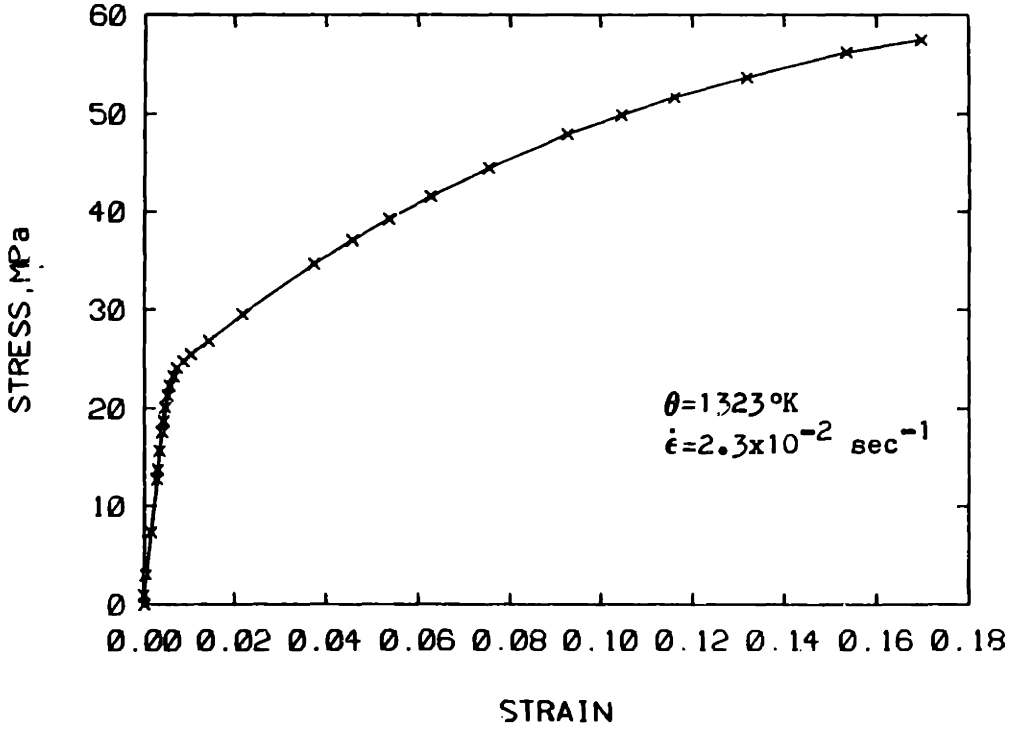

FIGURE 4.4.1 SIMULATION OF 1-D TENSION TEST WITH NO RECOVERY EFFECTS

shows, our method of integration uses about 2/3 less time steps than Euler's method. It is important to look at these graphs at how the distance between consecutive data points is smaller around the knee area of the stress-strain curve, and larger at the steady stress region of the same curve. This observation confirms that the automatic time step control mechanism is functioning properly.

In all the tests that follow, we will keep the isothermal, no recovery rate conditions, unless otherwise specified.

The second round of tests model a step loading-unloading-reloading condition, using two different strain rates. First, we use a positive strain rate $\dot{\epsilon}_1$, until we reach a strain of 8%, then we unload using $\dot{\epsilon}_1 = -\dot{\epsilon}_1$ until we reach a zero stress level. Then, we reload with a different and larger strain rate $\dot{\epsilon}_2$. The result of such a test is presented in figure 4.4.2. This test shows the procedures's ability to handle sudden changes in the sign of the loading condition. It can easily be seen that the data points behave in the form expected, changing fast enough to handle step changes in the load input, thus resulting in a smooth curve.

Figure 4.4.3 shows a series of tests that used a cyclic strain loading condition. The purpose of this particular test was to show how the strain-stress curve reach a steady

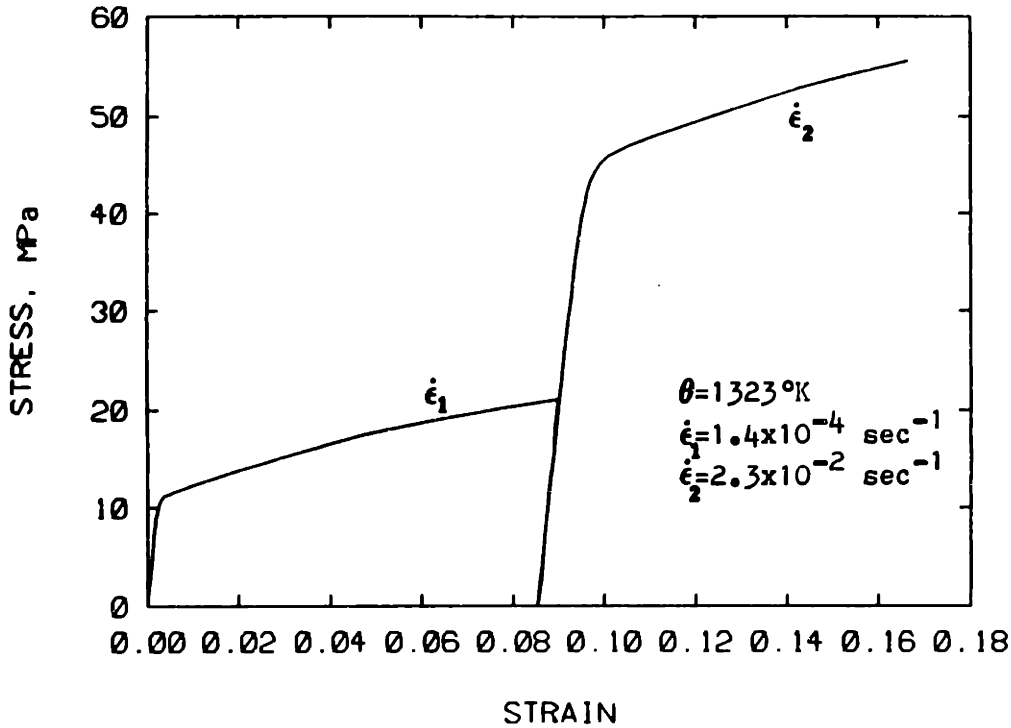

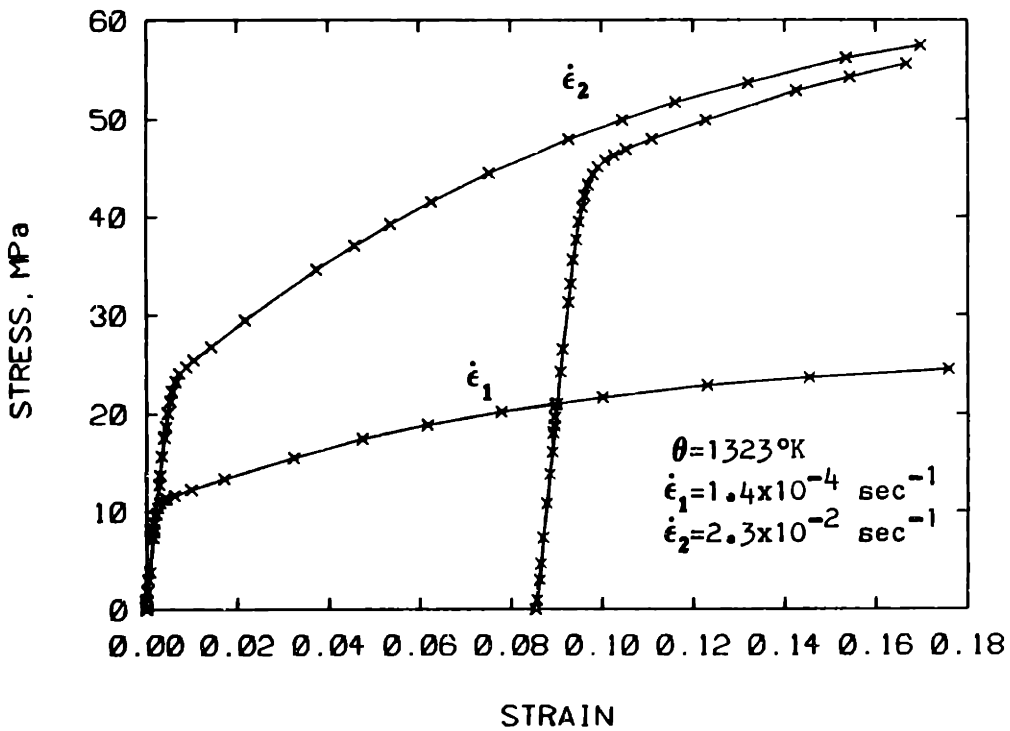

FIGURE 4.4.2 SIMULATION OF A LOADING-UNLOADING AND RELOADING TEST.

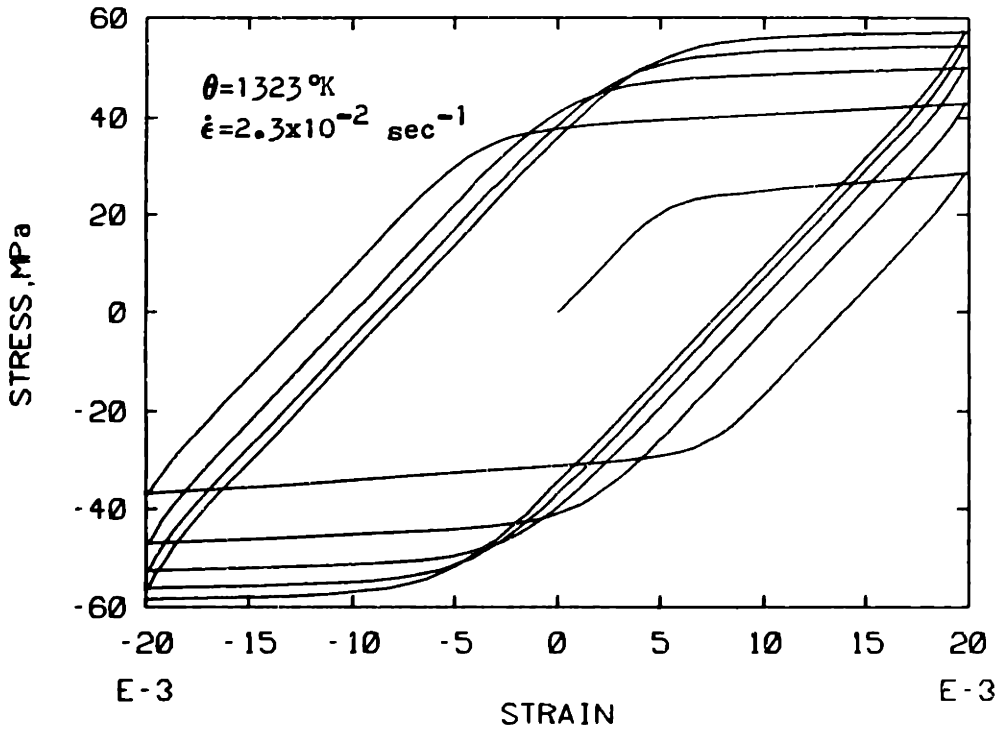

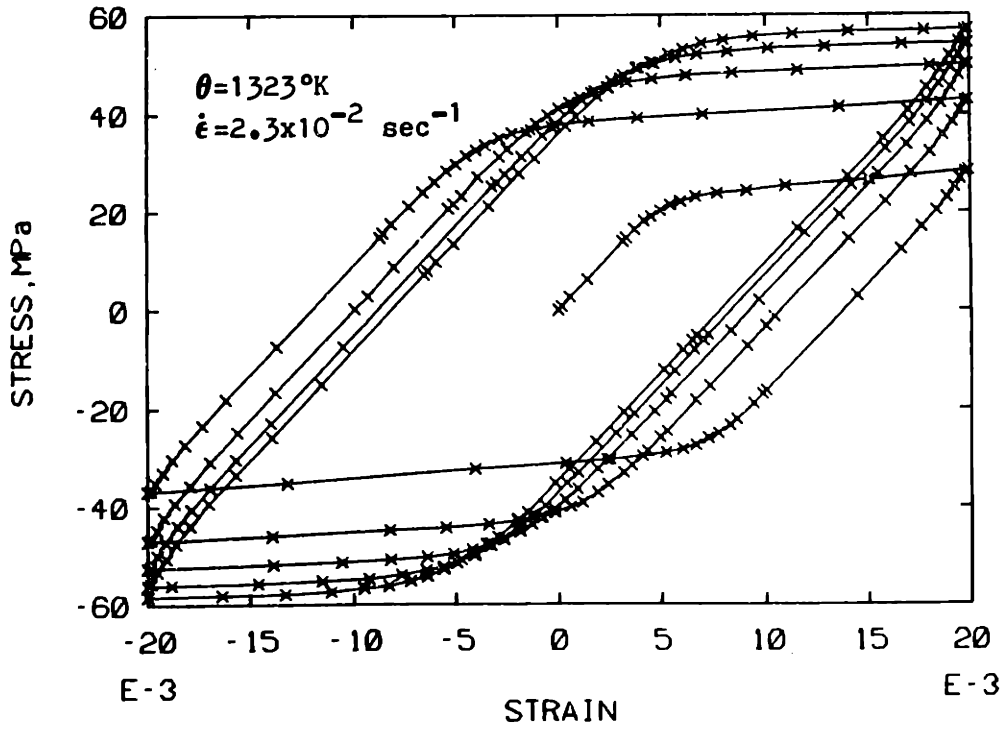

FIGURE 4.4.3 SIMULATION OF CYCLIC STRAIN LOADING TEST

state as the number of cycles increased. This behavior is due to the evolution of the variable s reaching a saturation value s^*. This rate dependent change needs to be handled by the numerical integration procedure in a effective way if any strain hardening effects are to be modeled. Once again, the numerical method works well reducing the time step at every region required in each and every cycle.

In the next series of tests, we have included the effects of static recovery ($r \neq 0$) and the effects of adiabatic temperature changes ($w=0.95$). The recovery rate r, as defined by equation 2.2.17, used the following parameters

$$p = 4.0$$

$$B = 9 \times 10^{-3}$$

which only represent a trial form of the recovery rate, as suggested by Anand and Parks [15]. This particular recovery rate form has not been proven to be the correct form corresponding to this material.

The first test which included the above conditions was a simple tension test at different strain rate levels. This test emphasized the effects of recovery rate and thermal rates when compared to a similar test where none of these effects were considered. The results from this comparisons are shown in figure 4.4.4 . In this figure, it can be observed how the curves with the mentioned effects included, reach a steady state stress much quicker. This is due to

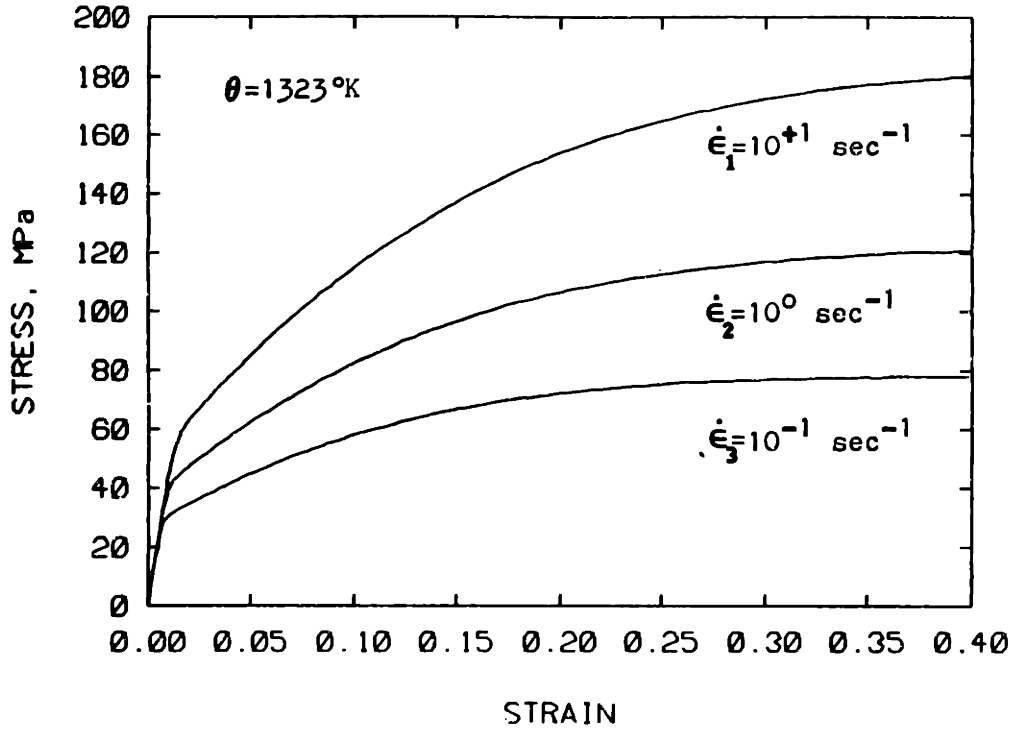

WITHOUT RECOVERY EFFECTS

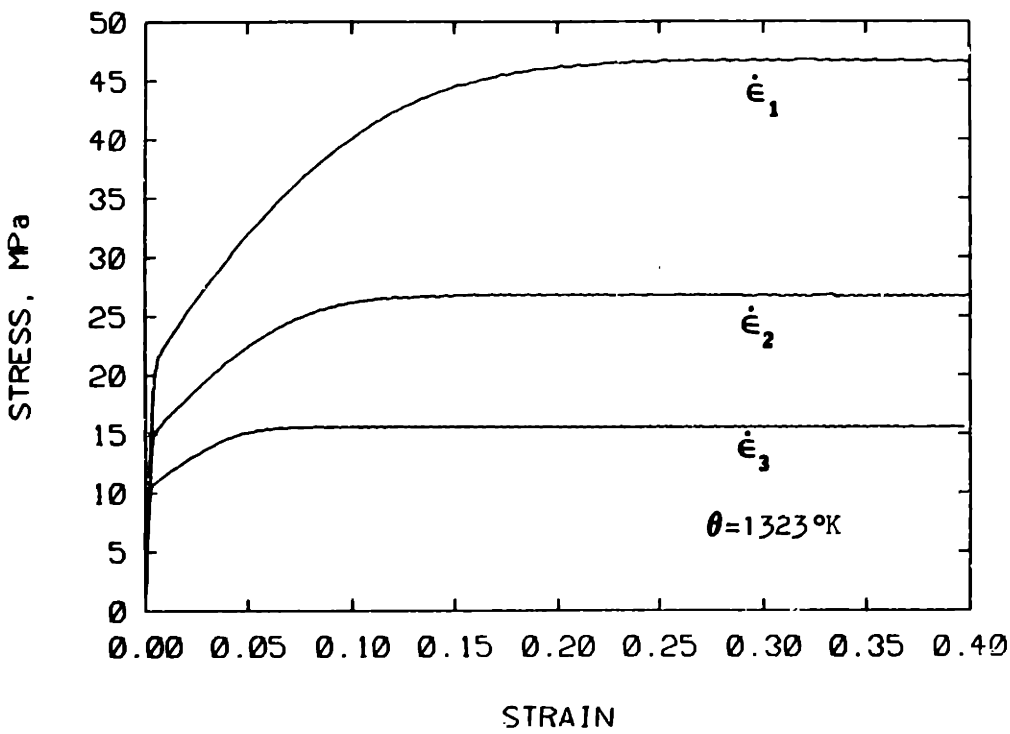

FIGURE 4.4.4 SIMULATION OF 1-D TENSION TEST WITH RECOVERY AND WITHOUT RECOVERY EFFECTS

the increased softening behavior introduced by the recovery rate. Looking at the region before the knee area, we notice that both sets of curves differ greatly as a result of the large effects of thermal recovery imposed by the non-isothermal condition. The introduction of recovery effects create large distortions which are not realistic since the trial form of r has not been proven, as explained in chapter 2. Also, it was noted that the inclusion of the recovery rate and temperature rate, increased the number of steps required to integrate the same strain range by about 3 times. This was due to the added non-linearities to the plastic strain rate equation. In figure 4.4.5, we can appreciate how the temperature and the internal variable s increase with time, for the corresponding strain rates shown in the last figure. It is important to note how the temperature rises faster for larger strain rates.

Finally, a large strain tension test shows how the temperature increase at large strain rates becomes so large that the stresess reach a peak and then they start to decrease.We attribute this to the big difference between the initial temperature and the higher final temperature. The thermal softening phenomena can be seen in figure 4.4.6 quite clearly.

These simulations were performed with the use of a FORTRAN subroutine, called HITREHO which includes our

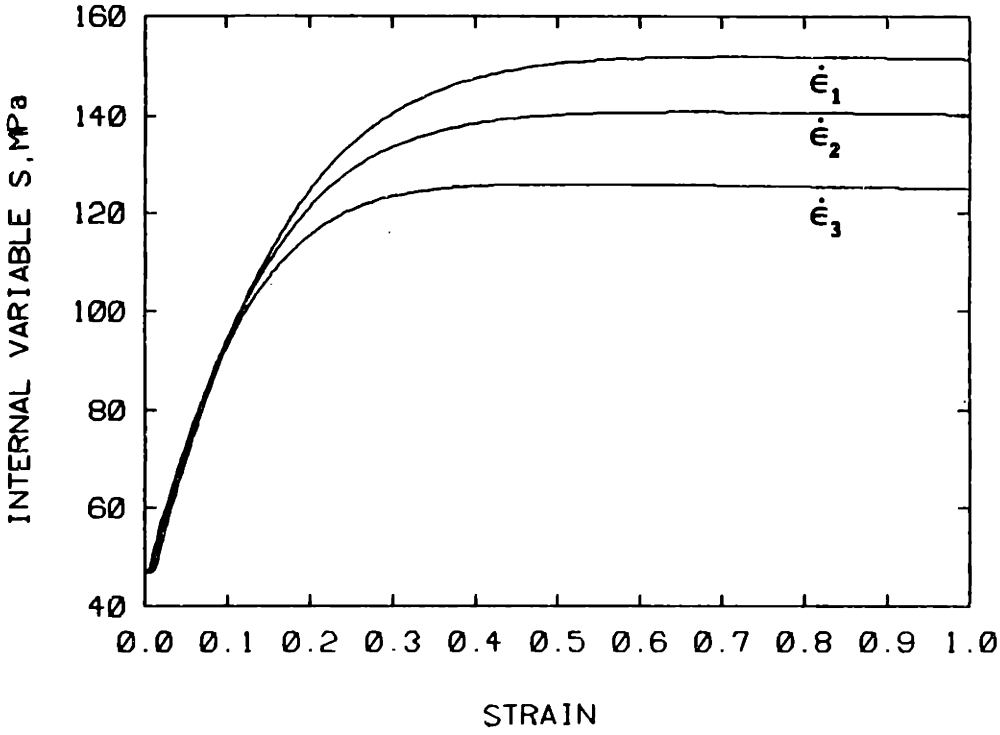

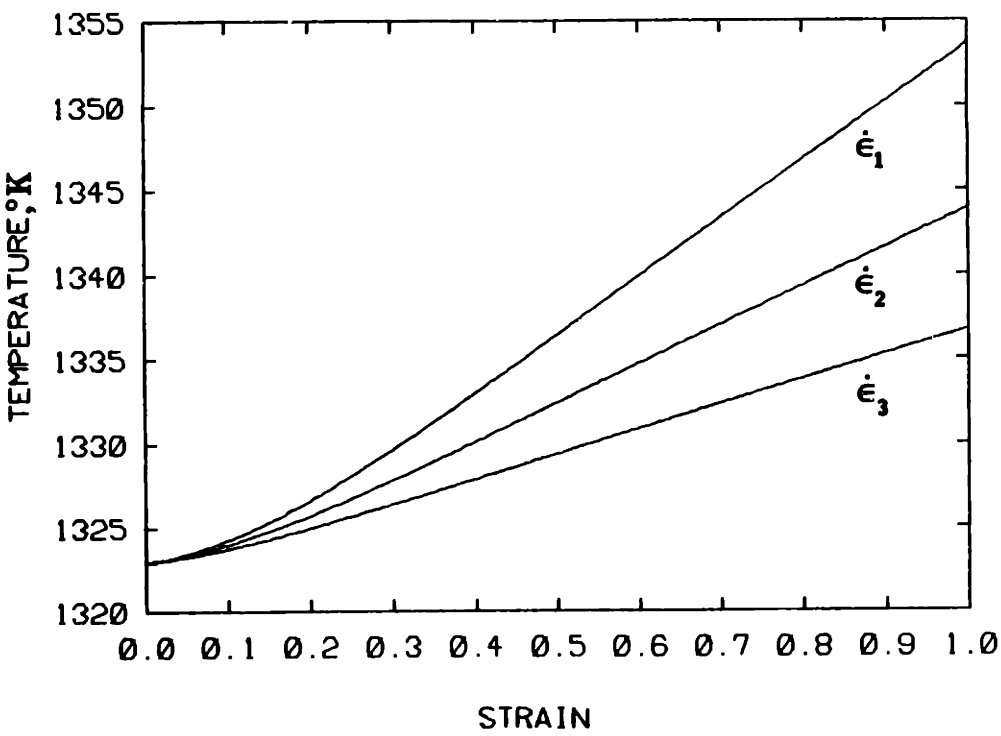

FIGURE 4.4.5 TEMPERATURE AND INTERNAL VARIABLE HISTORY

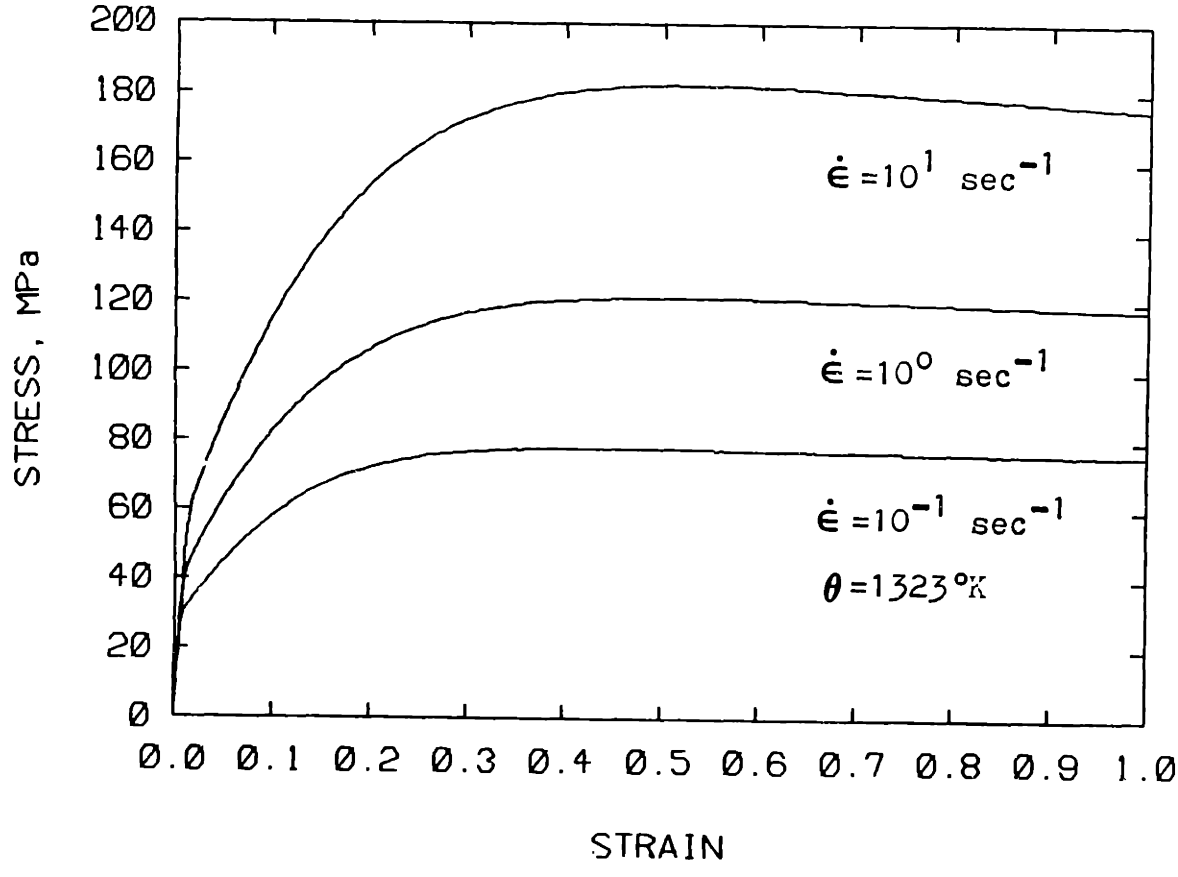

FIGURE 4.4.6 LARGE STRAIN RANGE TENSION TESTS

proposed numerical integration. The plots were performed using PENPLOT software, part of the Joint Computer Facility of M.I.T [16]. The mentioned subroutines can be found in appendix A.

4.5 CREEP SIMULATIONS

Using the constitutive equations presented in chapter 2, we now present simulations of several creep tests. These tests demonstrate the integration method's ability to model several kinds of rate dependent processes.

The first example simulates a simple creep test with a step stress input, as shown in figure 4.5.1. In this test, the load was aplied at two different stress levels, with no recovery effects included. The results of the strain history shows a very smooth curve, with a calculated savings of about 70% when compared to fixed time step integration methods. This is based on the amount of cpu time used in both cases. The results also show an accuracy good enough to the second significant digit when compared against classical models, such as the Euler forward method.

As a further example, using the same steel alloy, we modeled a single step stress creep when recovery effects were present. The results are shown in figure 4.5.2 . We

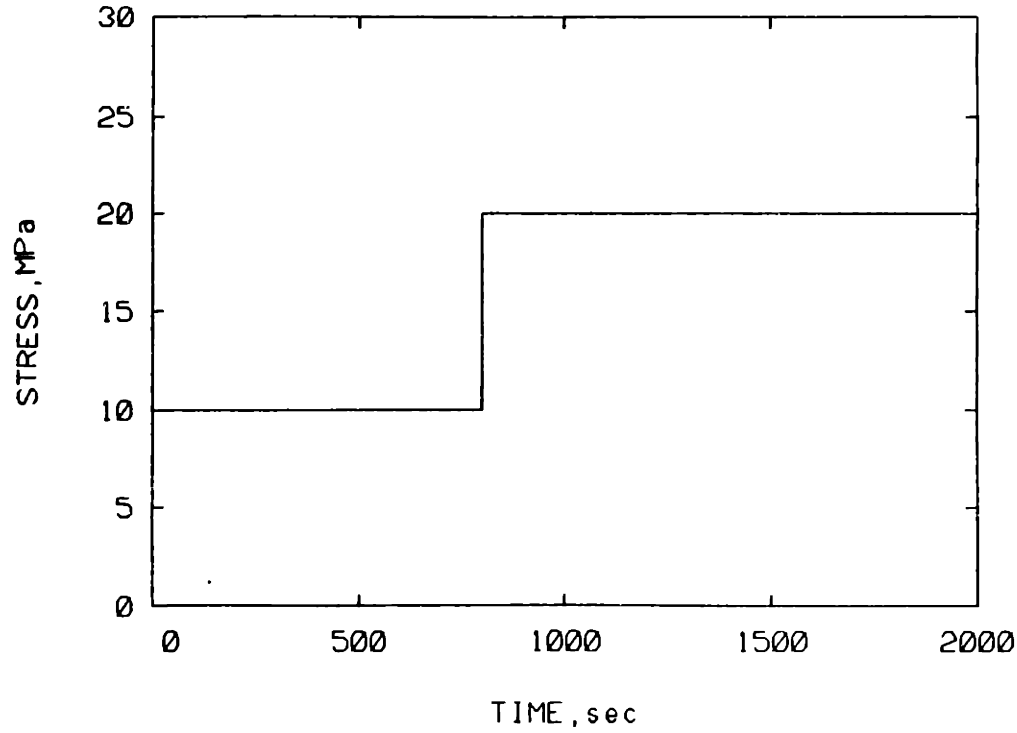

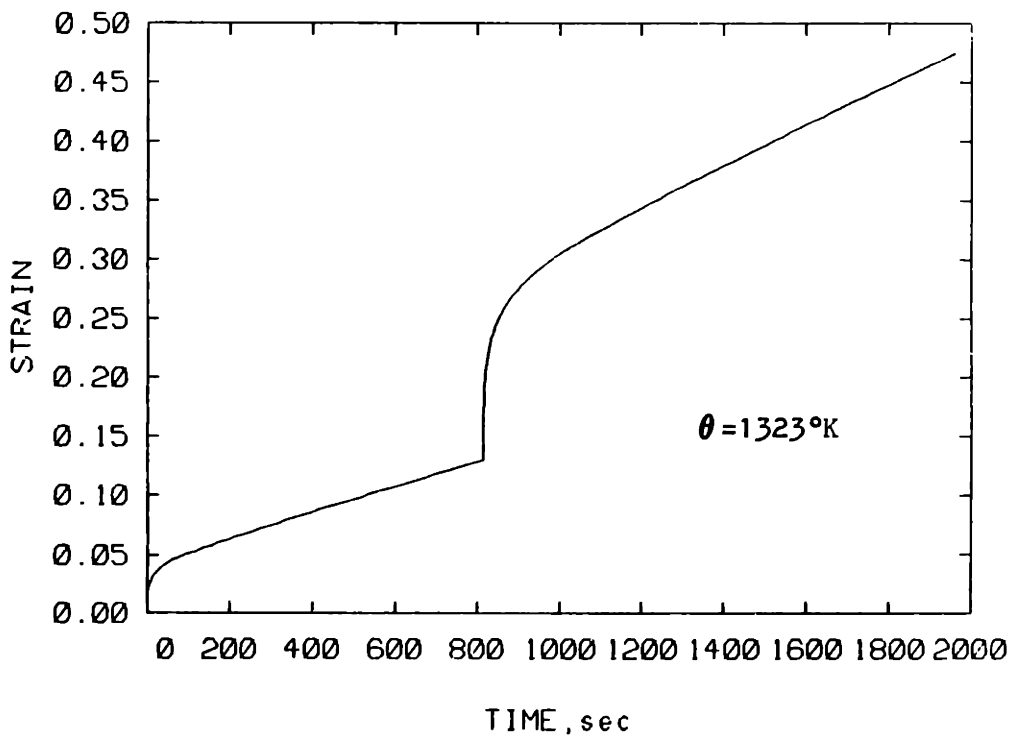

FIGURE 4.5.1 SIMULATION OF A STRESS JUMP TEST

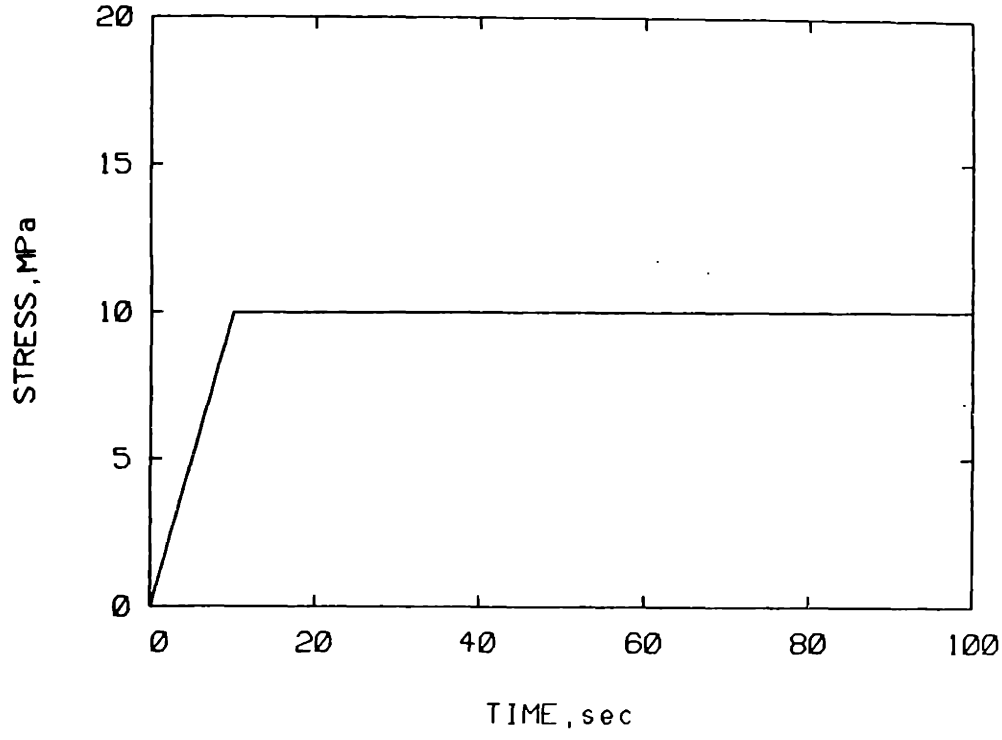

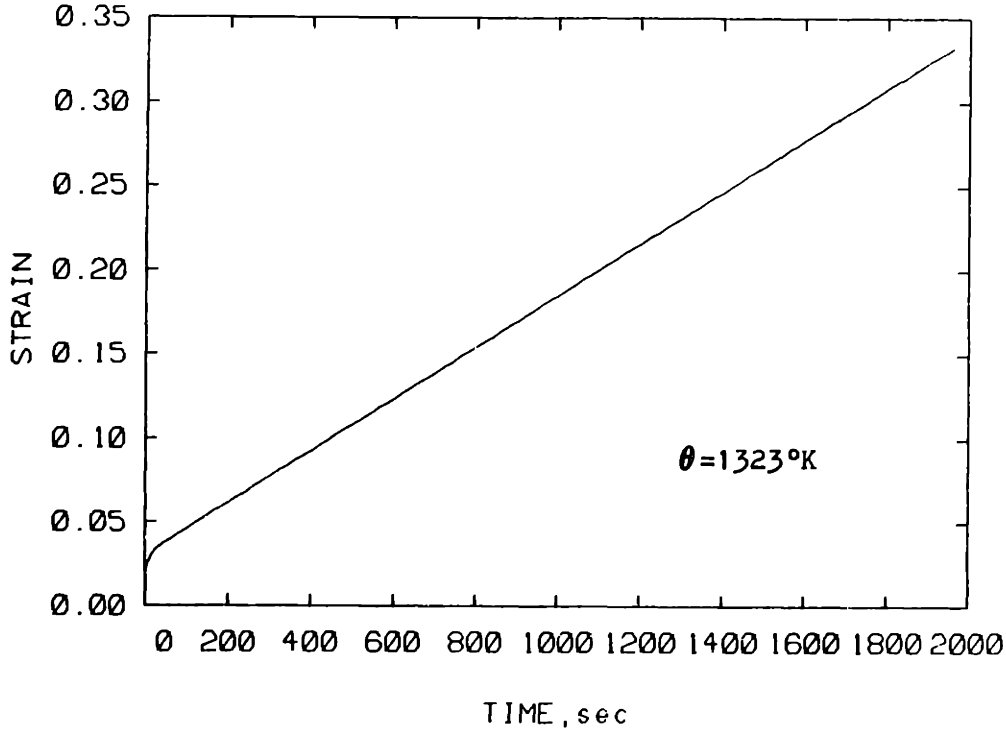

FIGURE 4.5.2 SIMULATION OF CREEP TEST WITH RECOVERY EFFECTS

used the same recovery parameters as the one presented in section 4.2. This time, we observe a strain value of about 30% after 30 minutes, when a stress level of about 10 MPa is maintained. This deformation seems resonable for the mentioned alloy at a temperature of about 1300^{o}K [17]. Also, in this test, the number of steps are increased due to the recovery effects introduced.

At this point, the integration method proposed in this thises performs very well when used to simulate simple one dimensional problems. It shows large savings when compared to other methods of integrations, while keeping the accuracy and stability within acceptable limits.

Chapter 5

NUMERICAL SIMULATION OF MULTIAXIAL PROBLEMS

5.1 INTRODUCTION

We now have shown how successful the integration method proposed in this research works in modelling simple one dimensional problems. However, in most real problems, more than one dimensional strain and stress are present and so, a more complex analysis must be done . In order to model multiaxial problems we used the finite element code ABAQUS. We have included a user material subroutine UMAT written by Professor Anand [18], which incorporates the elasto-viscoplastic equations that we have used during this research into ABAQUS. Also, this subroutine includes the time integration scheme proposed in this research.

In this chapter the incremental form of the elasto-viscoplastic equations used in UMAT, are derived. Also, several tests are performed to test the integration method's ability to model simple plane strain and axisymmetric problems. Also, a parametric study was made to

find the optimal values of the Ø-method's parameters.

5.2 INCREMENTAL FORM OF THE ELASTO-VISCOPLASTIC EQUATIONS IN 3-D

Using a similar procedure as the one used in section 4.2, we now present the incremental form of the 3-D constitutive equations. This derivation was performed by Anand [18] and its results were used to write UMAT.

The variables of interest at a future time t_{n+1} are

$$\tilde{\tau}_{n+1} = \tilde{\tau}_n + \Delta\tilde{\tau} \qquad 5.2.1$$

$$\underset{\sim}{\tilde{T}}_{n+1} = \underset{\sim}{\tilde{T}}_n + \Delta\underset{\sim}{\tilde{T}} \qquad 5.2.2$$

$$s_{n+1} = s_n + \Delta s \qquad 5.2.3$$

$$\theta_{n+1} = \theta_n + \Delta\theta \qquad 5.2.4$$

$$\gamma^p{}_{n+1} = \gamma^p{}_n + \Delta\gamma^p \qquad 5.2.5$$

To calculate the increment of the tensile plastic strain, we use

$$\epsilon^p = \gamma^p \underline{N} \qquad 5.2.6$$

where $\underline{N}$ represents the direction of the plastic straining. Since the calculations performed to derive the increments of equations 5.2.1 to 5.2.5 are excedingly long, we only present the final form of the stress increment, eq. 5.2.2. A full derivation of these incremental forms are included in

appendix B. Thus, we can write the increment of the Kirchhoff stress as

$$\Delta\tilde{\underline{T}} = [\,\bar{\underline{L}} - (\frac{\nu}{1+\nu})\frac{1}{G}\,\underline{M}\otimes\underline{M}\,]\,\Delta\epsilon - 3\kappa\alpha\Delta\theta\,\underline{1} - (\frac{f\,\Delta t}{1+\nu})\,\underline{M} + (\mu - \bar{\mu})\frac{1}{\tilde{\tau}^2}(\underline{T}'\cdot\Delta\epsilon)\,\underline{T}' \qquad 5.2.7$$

where $\bar{\underline{L}}$ is defined as

$$\bar{\underline{L}} = 2\bar{\mu}\,\underline{I} + (\kappa - (\tfrac{2}{3})\,\bar{\mu})\,\underline{1}\otimes\underline{1}$$

where $\bar{\mu}$ is defined as

$$\bar{\mu} = (\frac{1}{\mu} + \frac{1}{h_1})^{-1} \qquad 5.2.8$$

$$\nu = \phi\,G(PDA)\,\Delta t_n \qquad 5.2.9$$

The value of $\underline{M}$ is

$$\underline{M} = [\,(\frac{\mu}{\tilde{\tau}})\,\tilde{\underline{T}}'\,] \qquad 5.2.10$$

and

$$h_1 = \frac{\tilde{\tau}}{\phi\Delta t\,f} \qquad 5.2.11$$

Here, G is defined as

$$G = \mu - \left\{\frac{PDC\,(\omega/\rho C)\,\tilde{\tau} + PDB\,(HB)}{PDA}\right\} \qquad 5.2.12$$

and

$$HB = \frac{h}{1 + PDH} \qquad 5.2.13$$

The incremental form of the material equations presented were introduced in the material subroutine UMAT. In this way ABAQUS can take the increments of the stress

tensor and calculate from that the increments of the displacement. In ABAQUS, the spin terms of $\underline{\tilde{\tau}}^{\nabla}$, the Jaumman derivative of the Kirchhoff stress, eq. 2.2.3, are taken care by the main body of the program. A modified version of UMAT, to include the automatic time step control measures, is presented in appendix A.

5.3 PARAMETRIC STUDY OF THE Ø-METHOD

In this section we present the results of several parametric studies done with the time integration procedure proposed in this research. Such studies were done in order to find an efficient combination of **Ø** and **dt** to be used in the 3-D problems.

Toward this purpose we tried simulations of cases that approximated, in the best possible way, a 1-D tension test. This was done using a single axisymmetric element mesh. The possibility of necking is not allowed. To simulate a constant true strain rate, we wrote a user subroutine called DISP which translates the true strain rate to an equivalent displacement. The mesh for this case can be seen in figure 5.3.1. The ABAQUS input deck is found in Appendix C. The material parameters used are the ones corresponding to Fe-0.05% weight carbon steel, with the values found in table 4.3.1 .

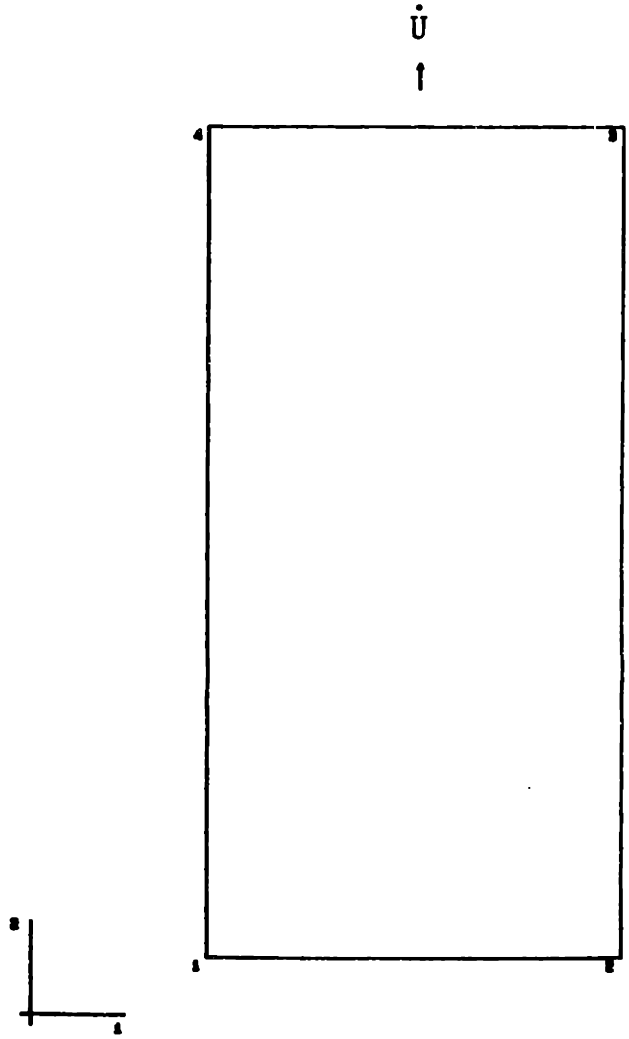

FIGURE 5.3.1 FINITE ELEMENT MESH FOR 1-D TENSION TEST SIMULATIONS

The first series of tests were done by comparing results from tension test simulations using ABAQUS, against experimental data obtained from [5]. The integration time step used, dt_o, based on the suggestions of section 4.4, is

$$\Delta t_0 = 0.05 \frac{s_0}{E \dot{\epsilon}}$$

and the values of $\emptyset$=0, 0.25, 0.5, 0.75, and 1. These comparisons are shown in figures 5.3.2 to 5.3.3b. As it can be observed, the model fits the experimental data fairly well. At this point, using a time step of dt_o, no difference can be noticed between the results corresponding to different $\emptyset$'s.

In order to check the effect of higher fixed time steps, we performed similar tension tests using different values of **dt** and different values of $\emptyset$. In each test, we fixed the time step to a multiple of dt_o and compared the data for different $\emptyset$ against a "base" curve. The base curve was computed with a fixed time step of dt_o and $\emptyset$=0. The first test uses a time step value of $2dt_o$. The results are ploted in figure 5.3.4 .As we can see, as the value of $\emptyset$ increased, the stress at the same strain decreased as compared to the base curve. This agrees with the implicit behavior of the integration method for $\emptyset$>0.0. Also, the accuracy decreases slightly since we use one half as many steps as the base curve. No oscillations of the solution

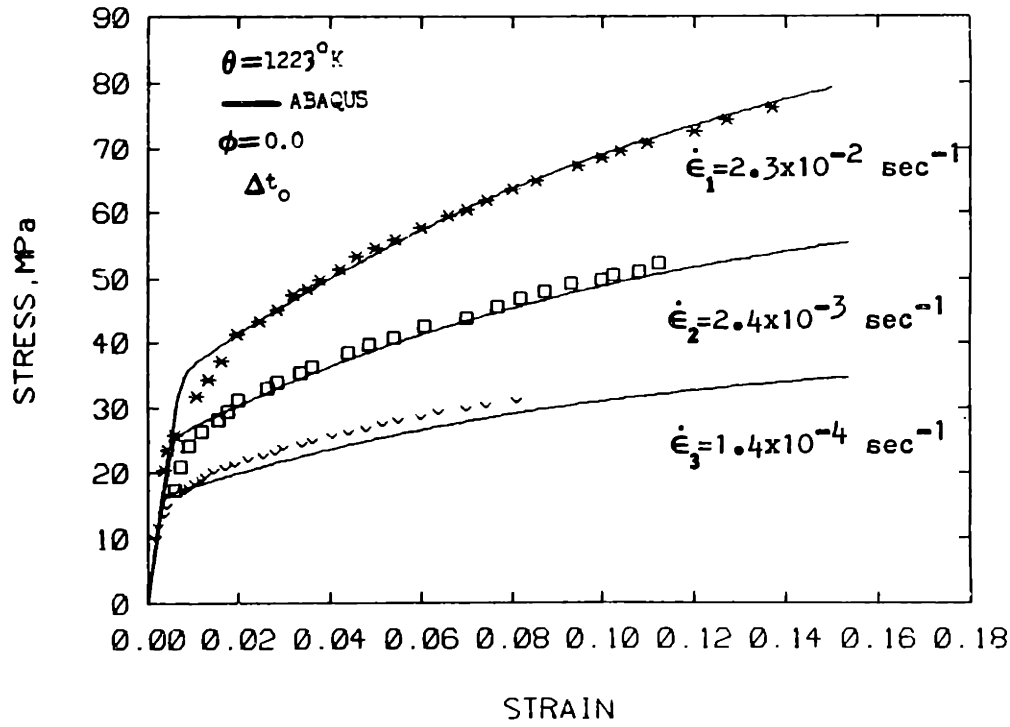

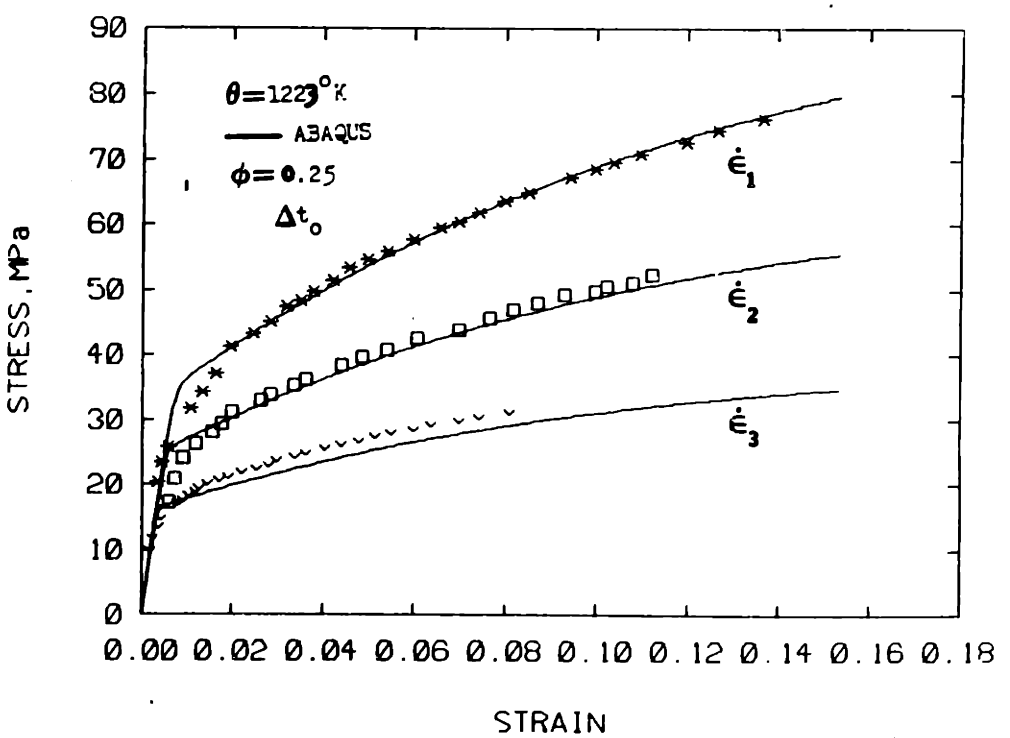

FIGURE 5.3.2 EXPERIMENTAL RESULTS AND ABAQUS SIMULATIONS OF UNIAXIAL TENSION TESTS

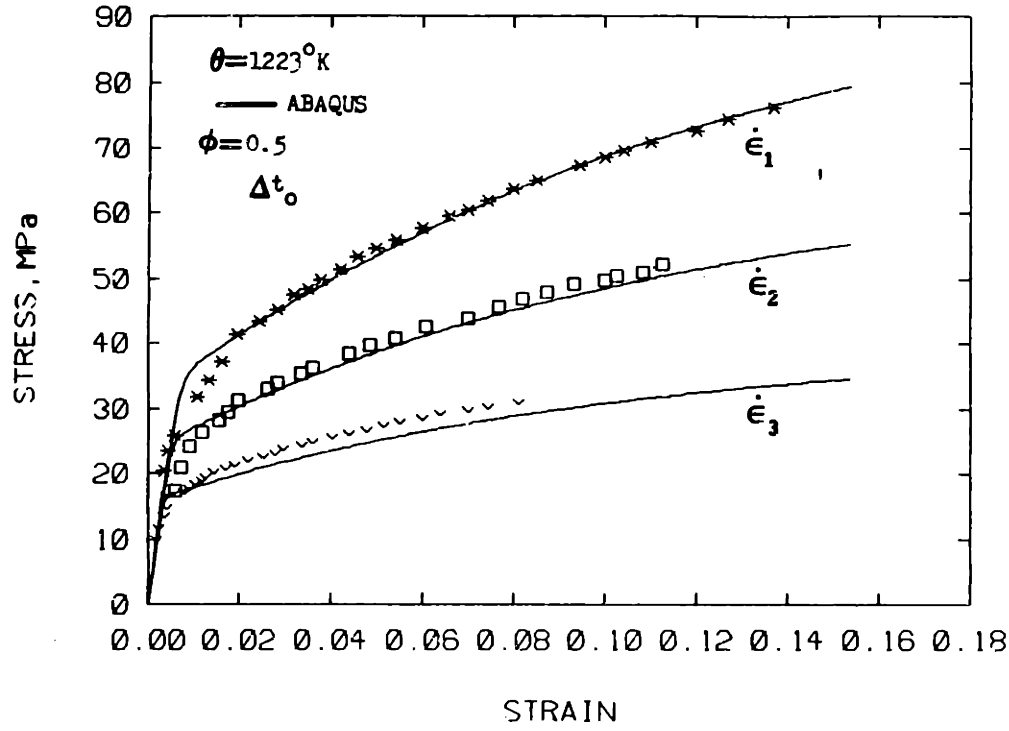

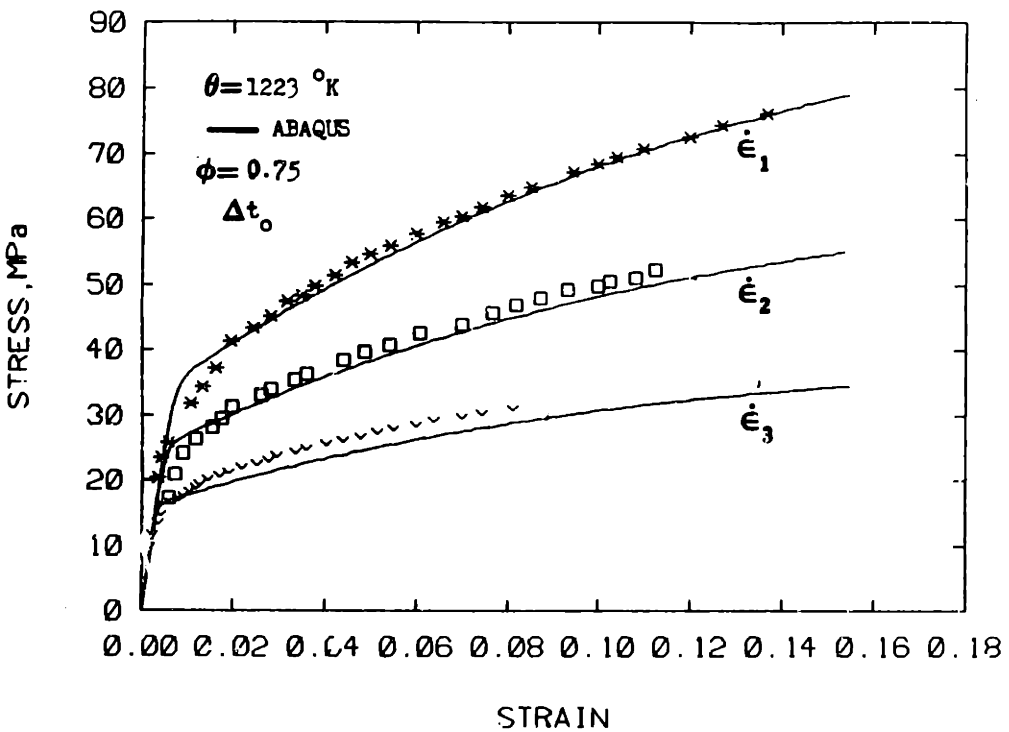

FIGURE 5.3.3 EXPERIMENTAL RESULTS AND ABAQUS SIMULATIONS OF UNIAXIAL TENSION TESTS

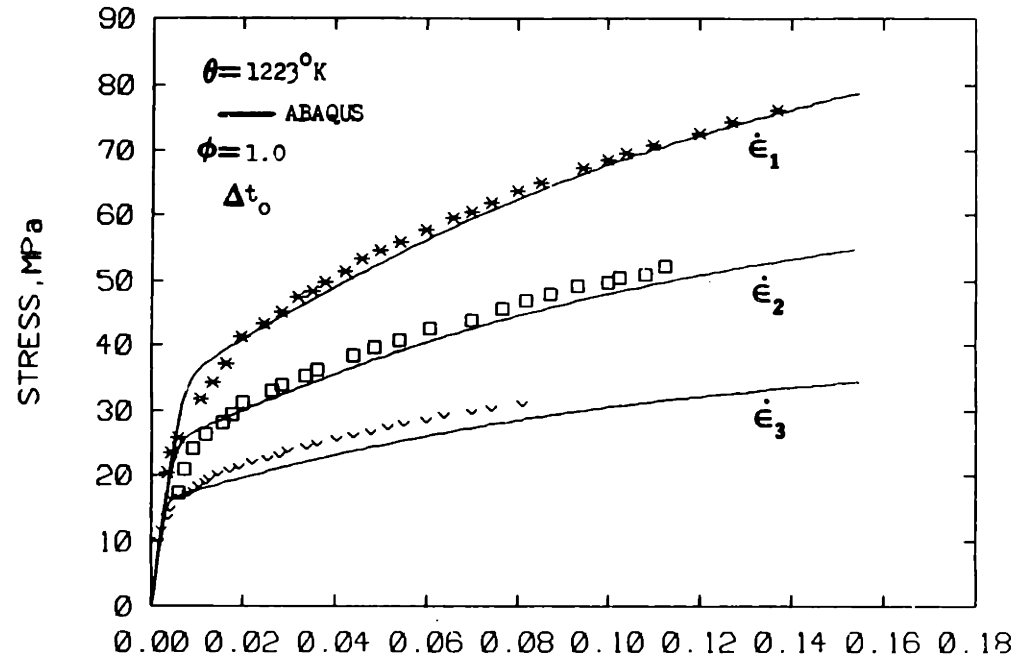

FIG 5.3.3b

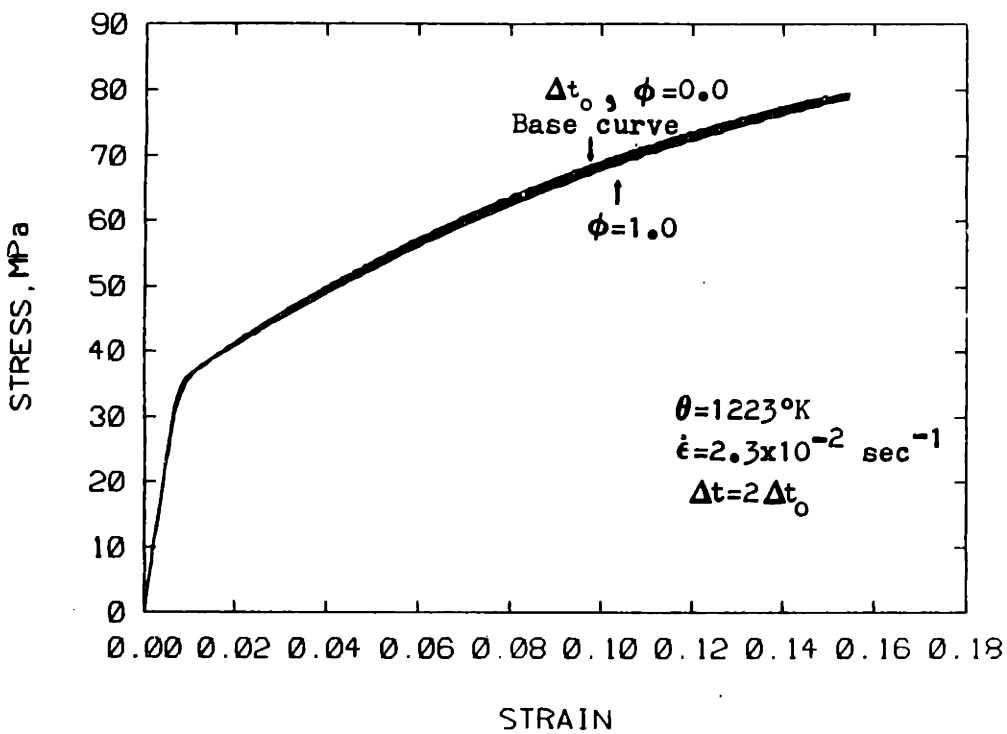

FIGURE 5.3.4 PARAMETRIC STUDY OF THE TIME INTEGRATION PROCEDURE

were noticed.

Next, using a fixed time step of $5dt_o$, we performed the same tension test. The results are ploted in figure 5.3.5a . As it can be observed, the accuracy becomes less than the previous test, and also, for the smallest value of $\emptyset$, $\emptyset$=0.25, the solution starts to oscillate slightly at the knee area. As expected, the solution remains very stable for larger values of $\emptyset$, but the accuracy obtained decreases respectively. Finally, using a fixed time step of $10dt_o$, we performed another tension test with the results obtained shown in figure 5.3.5b . This time, for almost all the values of $\emptyset$, the solution oscillates greatly, except for the value of $\emptyset$=1. Here the solution only oscillates a little at the knee region. The solution's accuracy becomes very poor for any of the values of $\emptyset$, but is extremely poor for $\emptyset$=1. Here, the trade off between accuracy and stability can easily be seen.

Finally, to test the method's behavior for the case of changing strain rates, we performed a cyclic strain rate test, using a fixed time step algorithm. After many trials, it was found that a combination of $\emptyset$=0.75 and a time step of $2dt_o$ yielded acceptable results. Compared to the base curve the test showed accurate results. The results from this comparison can be seen at figure 5.3.6 .

From all of the results obtained in this section, we

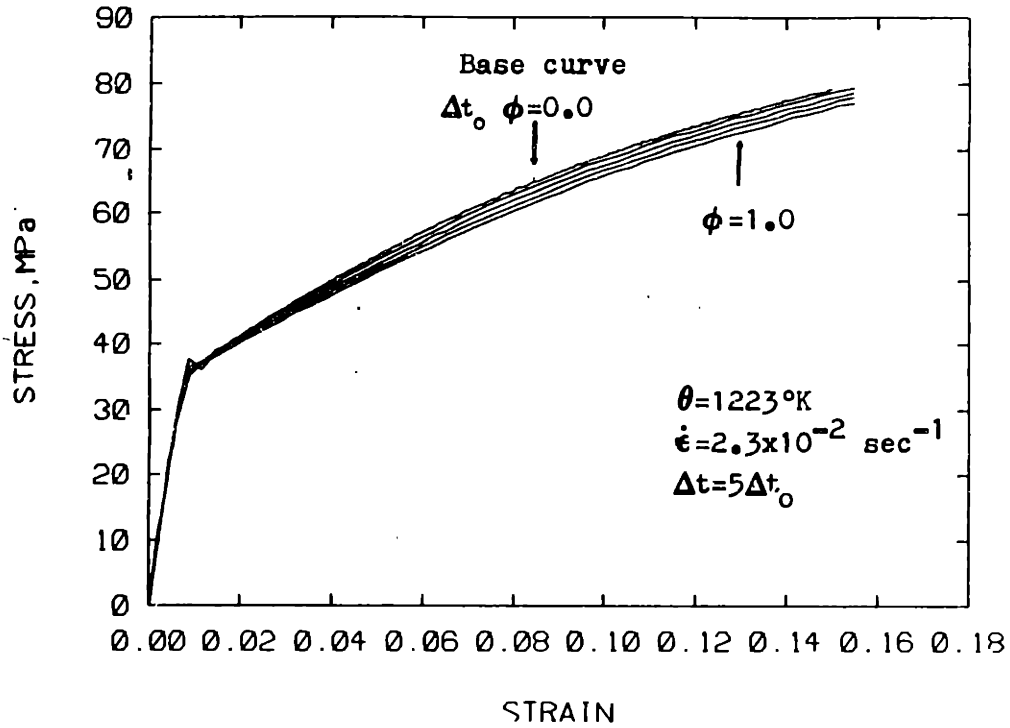

(a)

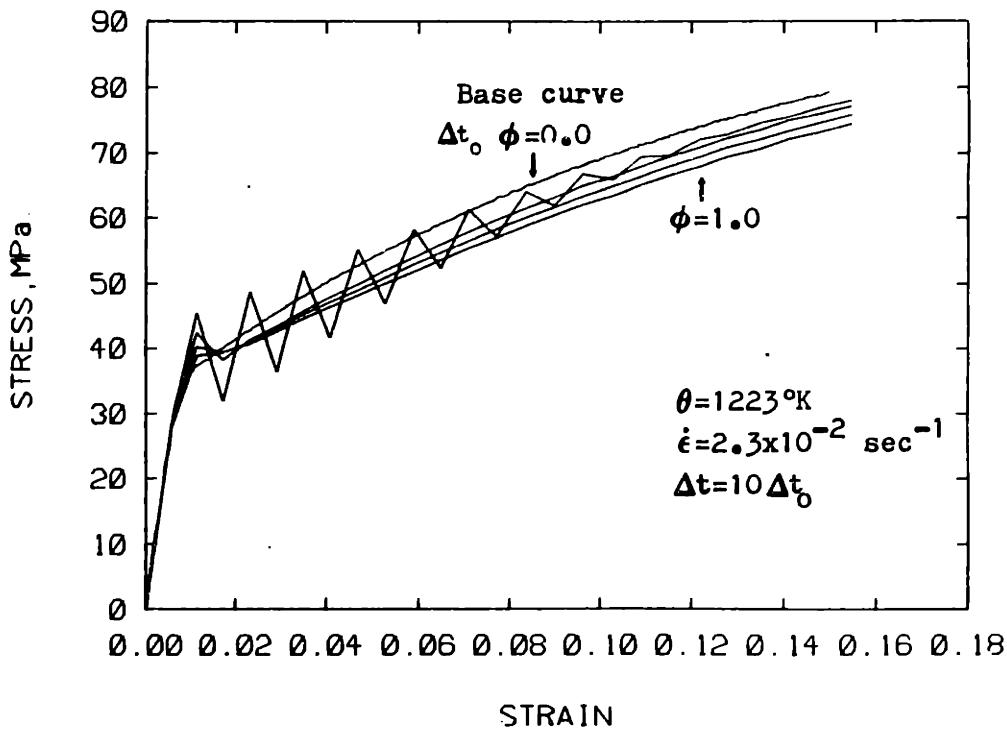

(b)

FIGURE 5.3.5 PARAMETRIC STUDY OF THE TIME INTEGRATION PROCEDURE

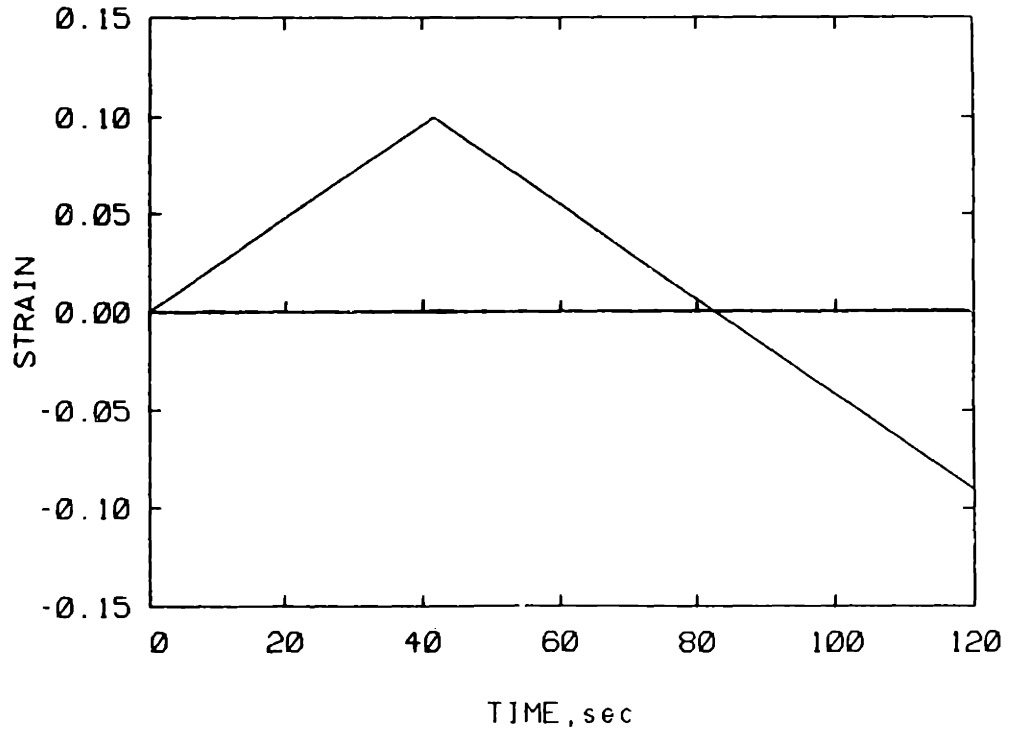

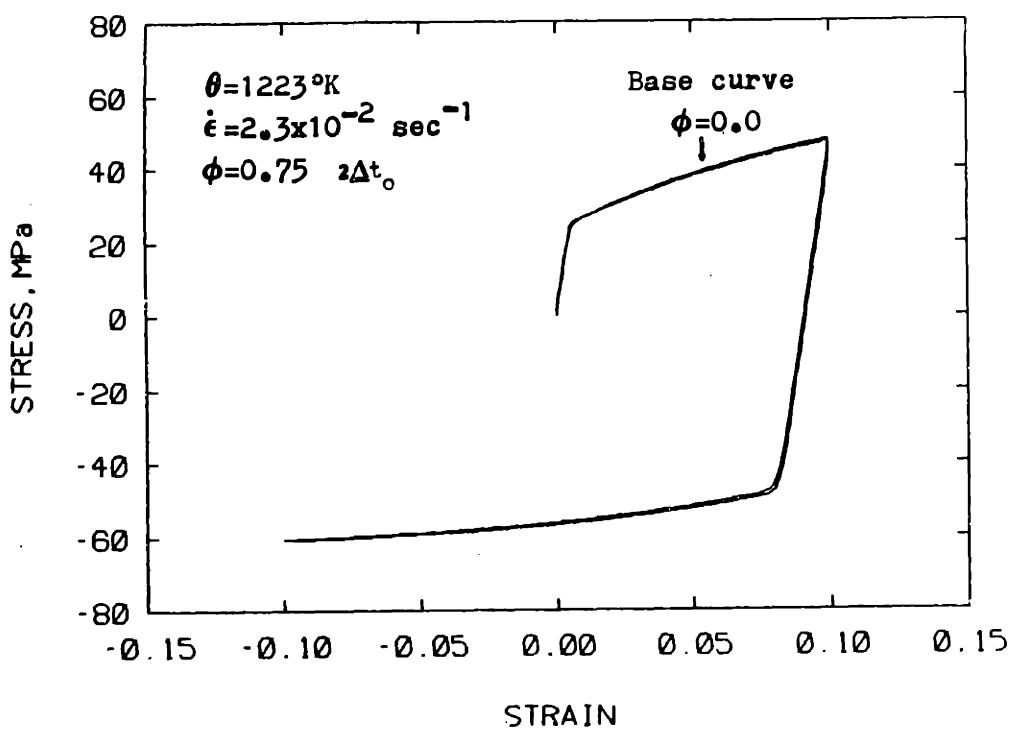

FIGURE 5.3.6 ABAQUS SIMULATION OF A CYCLIC STRAIN LOADING TEST

conclude that a good parameter combination set to use with the Ø-method is

$$\phi = 0.75$$

$$\Delta t \leq 2\Delta t_0$$

where **dt** represents the maximum time step that can be used in areas of large stiffness, such as the knee area.

5.4 AUTOMATIC TIME STEP CONTROL USING ABAQUS

In order to test the time integration procedure proposed in this research with 3-D problems, we also made use of the automatic time step control included in ABAQUS [2].

The automatic time step control procedure used in ABAQUS is almost the same to the one we have outlined in section 4.3, with the exception of how the algorithms handles the consecutive time step incrementation. The ABAQUS automatic time step control uses a more conservative incrementation of the time step in order to handle very stiff equations. The integration scheme outlined in this research will be used by ABAQUS, by means of the routine UMAT.

The first test series were done for three different tension tests using a constant true strain rates. These

results were compared against the results from section 5.3, and against experimental data. This comparison is shown in figure 5.4.1. We see that the results of both tests are fairly close, with the difference being that the run using the automatic time step control used only 60% of the CPU time that the fixed step run used. Thus, savings of up about 40% in total Cpu time were obtained. The values of **CETOL** and $\mathbf{dt_o}$ are the same values as the one defined in section 4.3 and 4.4. We have also introduced a constrain in the maximum time step allowed in order to obtain reasonably accurate results. The parameters used are

$$\Delta t_0 = 0.01 \frac{s_0}{E \dot{\epsilon}} \qquad \text{CETOL} = 0.01 \frac{s_0}{E}$$

$$\Delta t_{max} = 15\ \Delta t_0$$

The next series of tests were performed using a cyclic loading history, using true strain rate cycles. Using the above parameters for the integration procedure, we compared results of the automatic time step control integration against it's fixed small time step counterpart, $\mathbf{dt=2dt_o}$ and $\mathbf{\emptyset}$=0.0. We can see the results in figure 5.4.2. Again, the results are very close to the base curve, and with a calculated Cpu time savings of about 50%.

After proving the automatic time step control's potential integrating one dimensional problems using ABAQUS, we can now proceed and model much more complicated problems that require multiaxial capabilities.

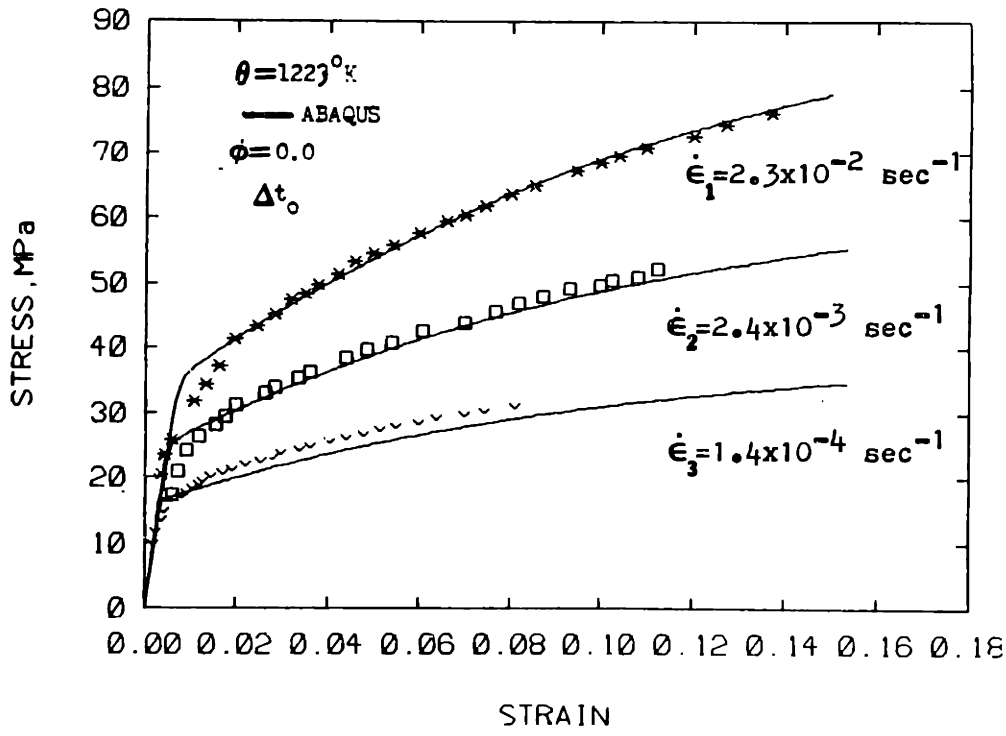

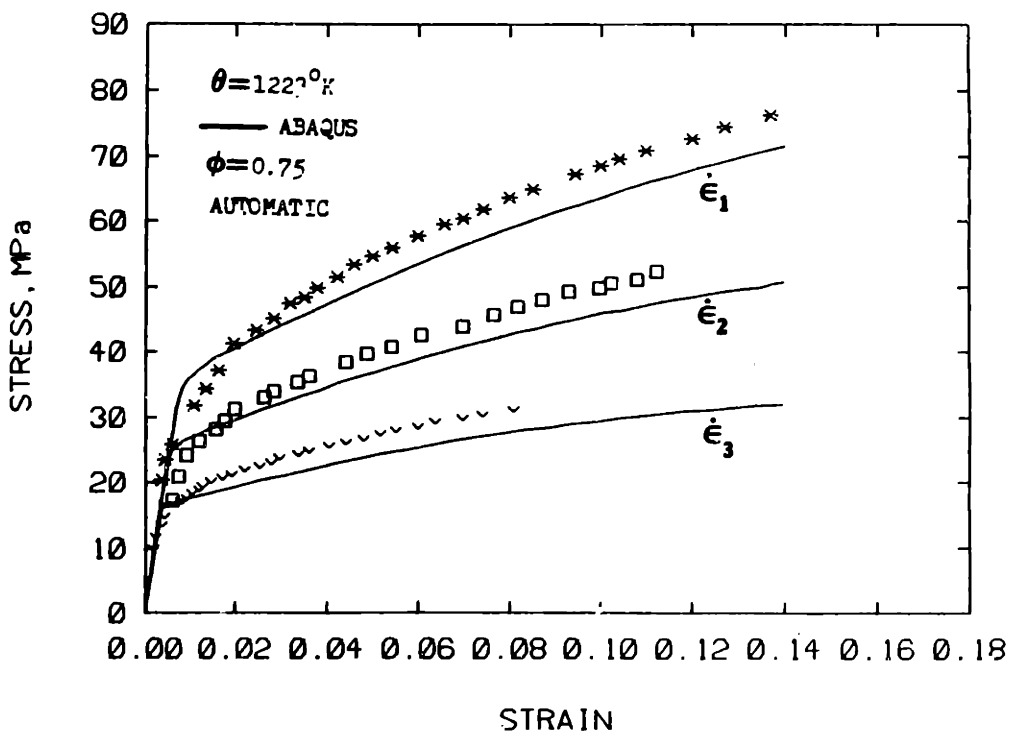

FIGURE 5.4.1 ABAQUS SIMULATIONS OF UNIAXIAL TENSION TESTS WITH AUTOMATIC AND FIXED TIME STEP INTEGRATION

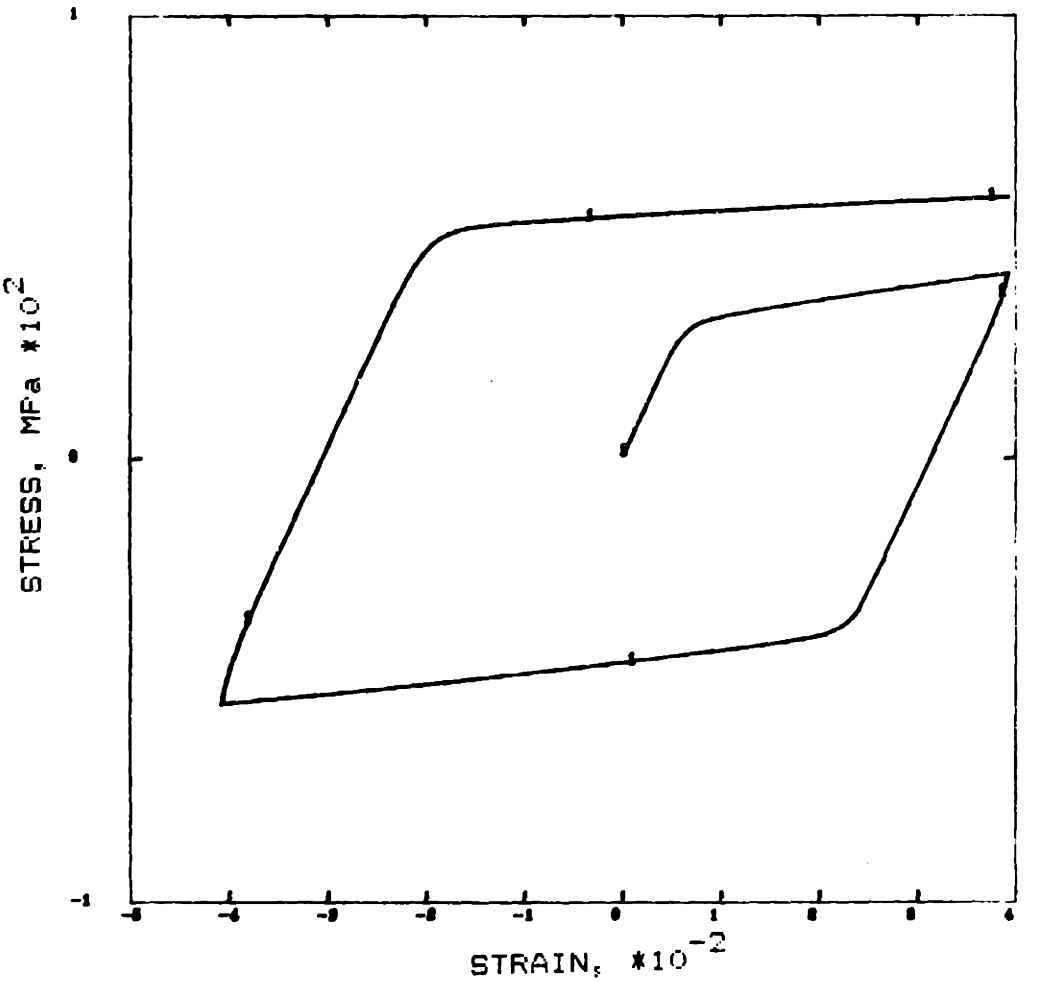

FIGURE 5.4.2 ABAQUS SIMUALTION OF CYCLIC LOADING TEST USING AUTOMATIC INTEGRATION

5.5 UPSETTING OF A CYLINDRICAL BILLET

A simulation has been done to show the solution of a 3-D case involving an axisymmetrical problem. This example should give an idea of the great effectiveness of the integration method to solve elasto-viscoplastic behavior.

The problem consisted of upsetting a cylindrical billet made of steel, which was reduced by 50% of its original length. The equations for hot working processes were used with no recovery effect, but with the inclusion of plastic work heating (w=0.9). This problem is of great interest for the manufacturing industry, especially when too high of a temperature rise may degrade the material [19]. Also, for this example, we used the assumption of adiabatic material behavior.

The mesh used in this analysis can be seen in figure 5.5.1. Only the top half of the cylinder is shown. Axisymmetric elements with reduced integration were used, CAX8R, to model this example. The die was modeled as a perfectly rigid surface which is completely rough. The material equations were introduced by means of the UMAT subroutine. The material parameters correspond to the steel alloy used throughout this research.

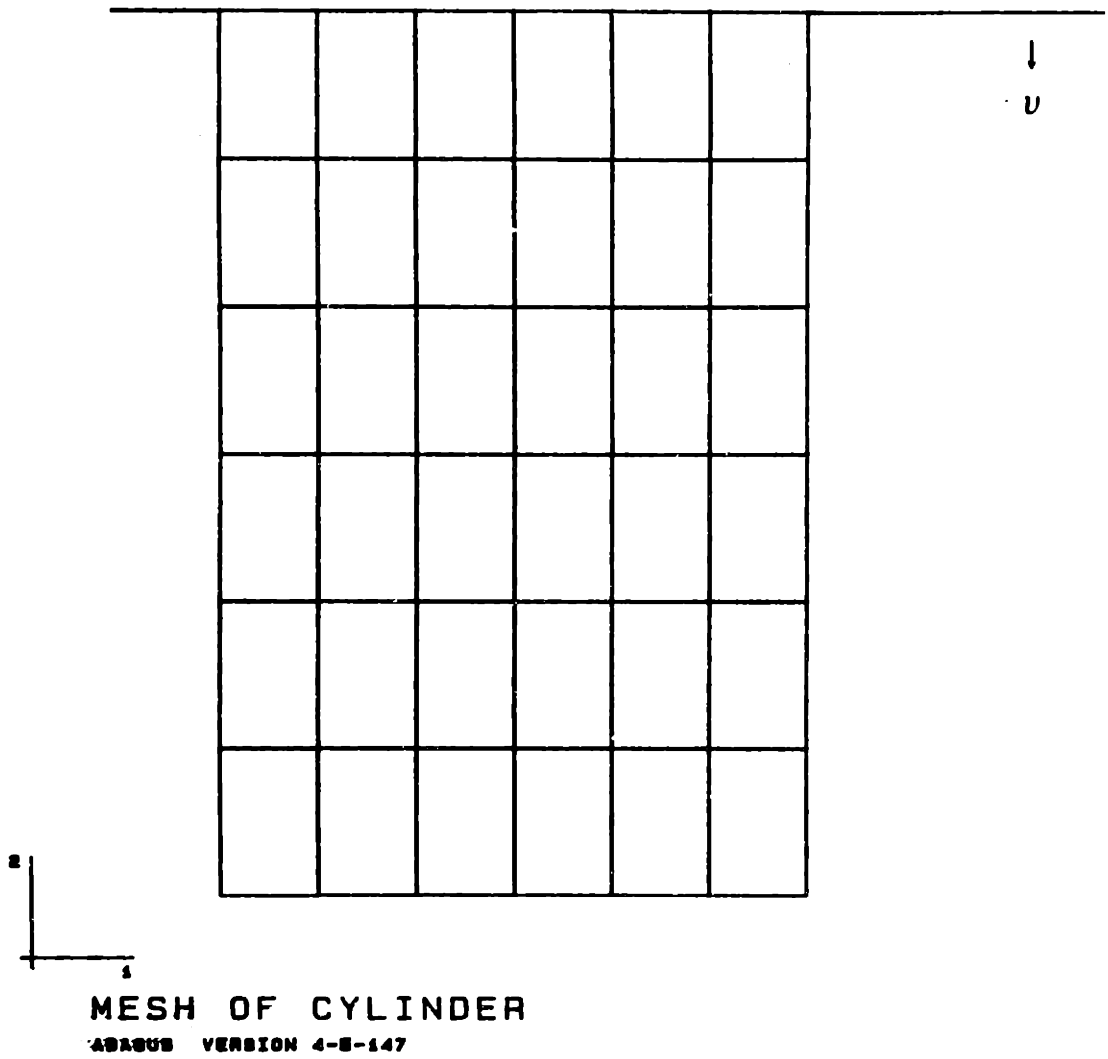

FIGURE 5.5.1 FINITE ELEMENT MESH OF A CYLINDRICAL BILLET

The analysis was performed using a slow upsetting, where the 50% reduction of length took about 100 sec. The die had a constant velocity to match this upseting. The minimum value of **dt** that was used is **dt**=1.0 sec.

The results of this analysis can be seen in figures 5.5.2 to 5.5.4 . The first figure shows the deformed configuration after the 50% reduction had taken place. The following figures show the distributions of the plastic strain and temperatures along the cylinder's interior. As it can be observed, peak strains of about 170% are found in regions close to the center of the cylinder, and a temperature rise of about $10^{o}K$ in the regions close to the center of the cylinder.

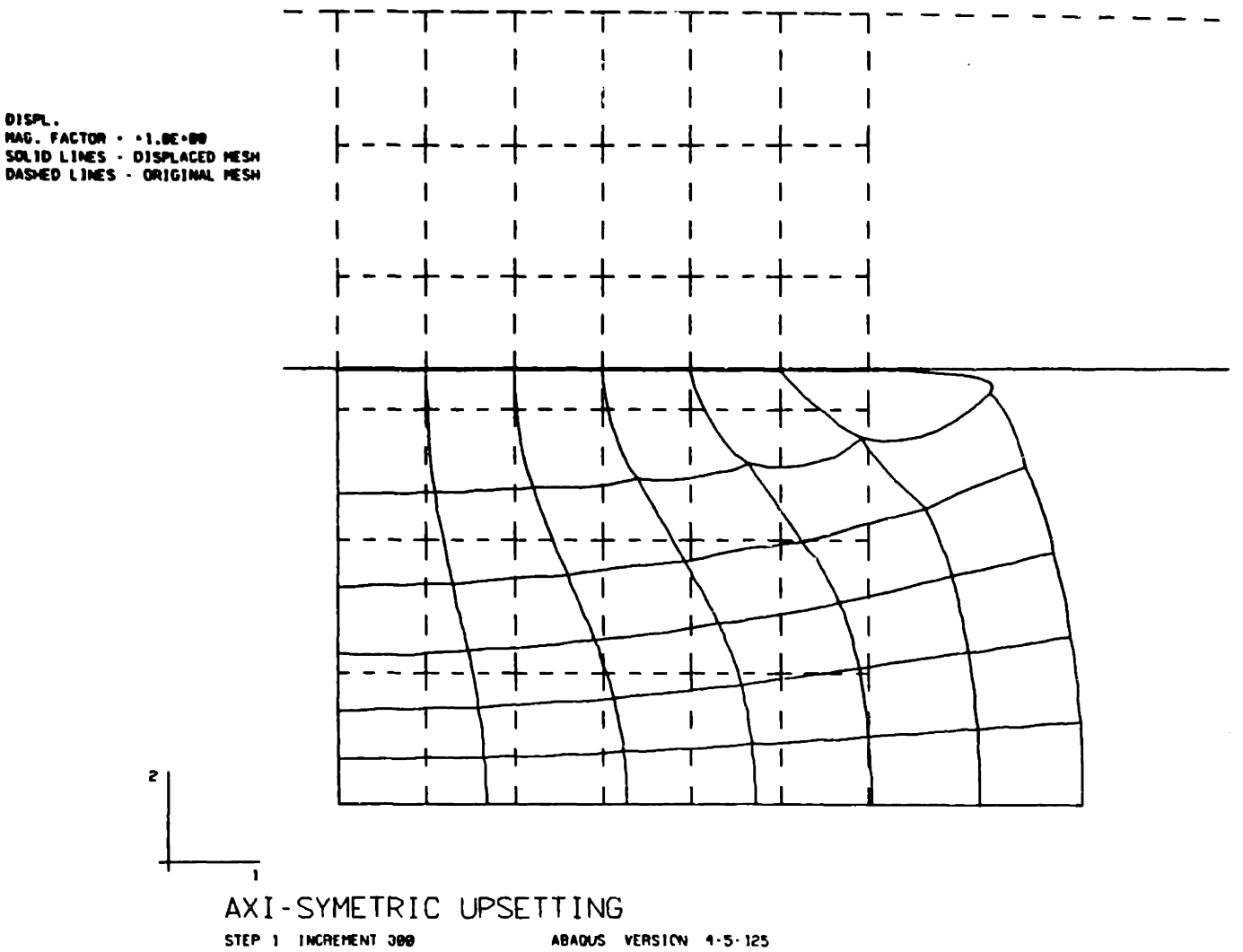

FIGURE 5.5.2 DEFORMED CONFIGURATION OF AN UPSETED CYLINDER

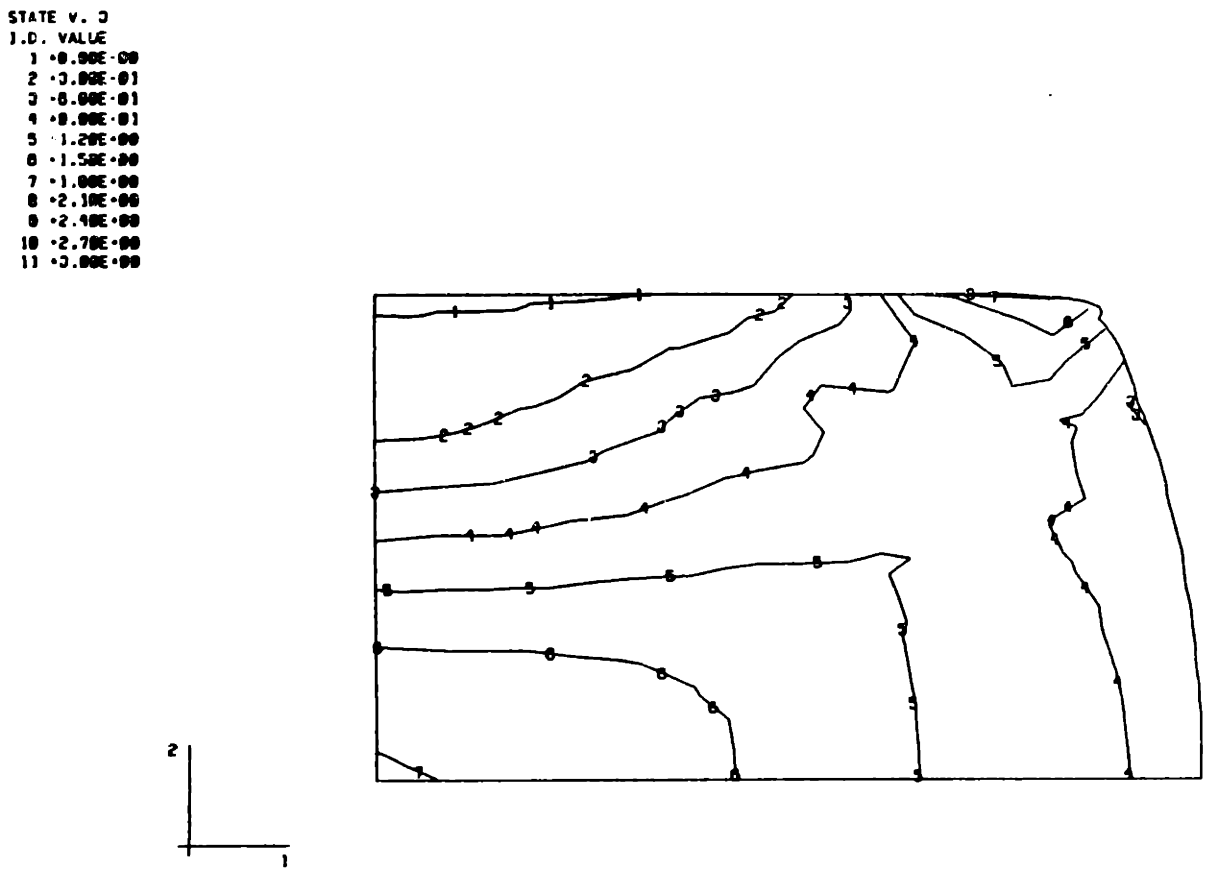

FIGURE 5.5.3 PLASTIC STRAIN CONTOUR OF THE DEFORMED CYLINDER

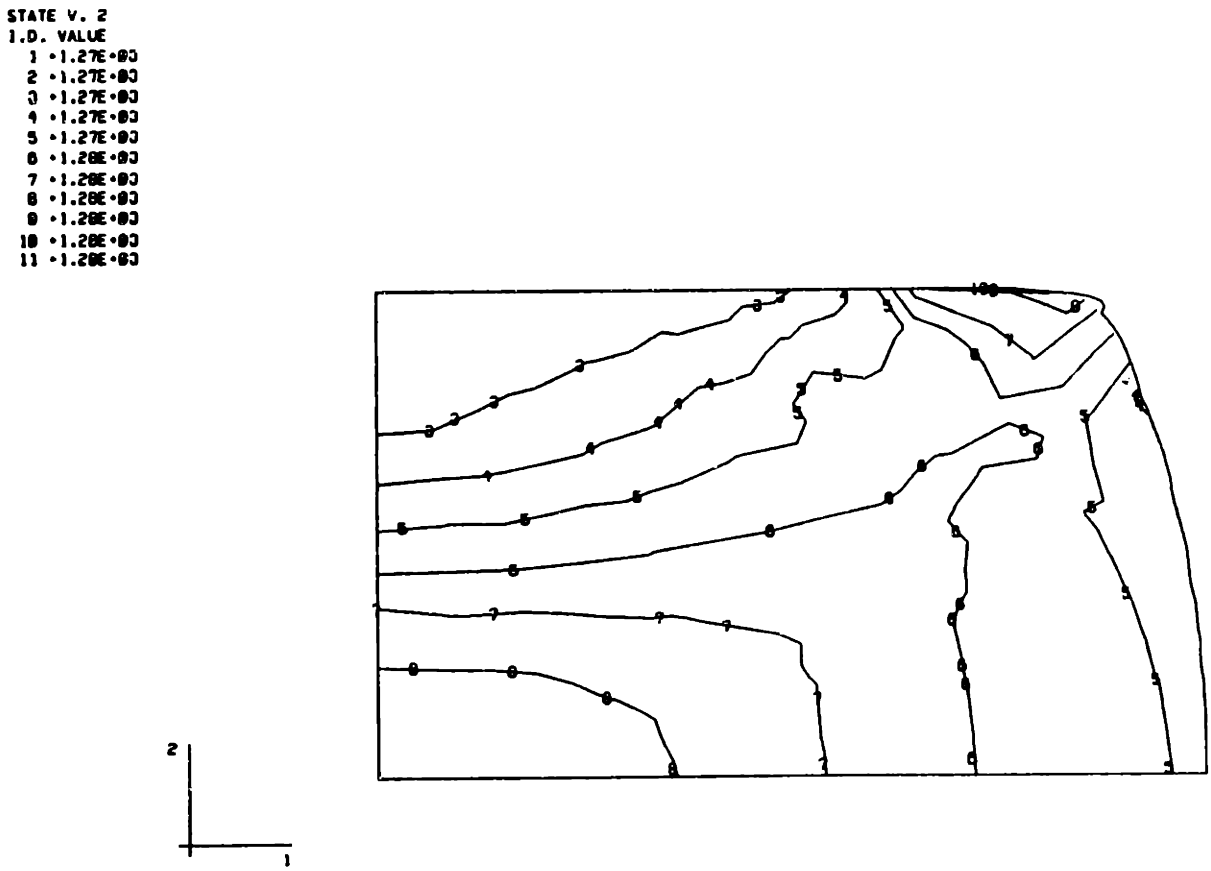

FIGURE 5.5.4 TEMPERATURE CONTOUR OF THE DEFORMED CYLINDER

Chapter 6

CREEP OF THICK WALLED CYLINDER UNDER INTERNAL PRESSURE

6.1 INTRODUCTION

Creep represents an important phenomena which is present in metals at elevated temperatures, when subject to a load. We now present the experimental results of a creeping thick walled cylinder subjected to a constant internal pressure. The experimental results are compared to results obtained from numerical simulations using the time integration technique developed in this research.

6.2 PROBLEM DESCRIPTION

The analysis of a thick walled cylinder under a constant internal pressure constitutes a classical problem in Creep theory. If the cylinder's material is exposed to a constant temperature higher then 0.4 times the material's

melting temperature, a creep behavior can be observed if a load condition exists. The secondary steady state creep behavior can be modeled for some specific materials, at least approximately, by using a power law model of the form

$$\dot{\bar{\varepsilon}}^{c} = A\,\bar{\sigma}^{n} \qquad 6.2.1$$

where the creep strain rate is expressed as a function of the stress and the material's constants **A** and **n** [17]. The above relationship implies a linear behavior between strain and time, for secondary creep only.

The theoretical solution for the creeping thick walled cylinder is a standard creep problem . This solution is summarized in Appendix D.

With the help of the equations presented in Appendix D, and with the equations of continuum mechanics, we are able to find approximate values of the parameters **A** and **n** from experimental measurements. It can be shown analytically that having two sets of measurements, at different pressure levels, the mentioned parameters can be obtained, given the power law nature of eq. 6.2.1. .Using these parameters, we should be able to reproduce the experimental results by means of a finite element simulation using the time integration technique presented in this research.

6.3 EXPERIMENTAL PROCEDURE

The experimental setup was designed having in mind the assumptions made in the analysis given in Appendix D. We used a 1" gauge length sample of 60-40 Pb-Sn Vaculoy Solder cylinder with an inside radius of **a**=0.1" and an outside radius of **b**=0.2". The cylinder was locked into a special support with two locking nuts which provided the constrains required to simulate the plane strain condition, as seen in fig. 6.3.1 . The bottom part of the cylinder was connected to an oil pump, which supplied the internal pressure required. Once the pressure was ramped to the desired level, we kept it constant and recorded the changes of the outside diameter at fixed intervals of time. This experiments were conducted for three different internal pressures of 600,700 and 800 psi. For each pressure, we recorded data until the cylinder burst.

60-40 Pb-Sn Solder was selected because at room temperature it is already above half its melting temperature. No tests were done to find the basic material parameters, such as elastic moduli, for the specific alloy used. These parameters are assumed to be very close to the properties available for this alloy in the literature [20].

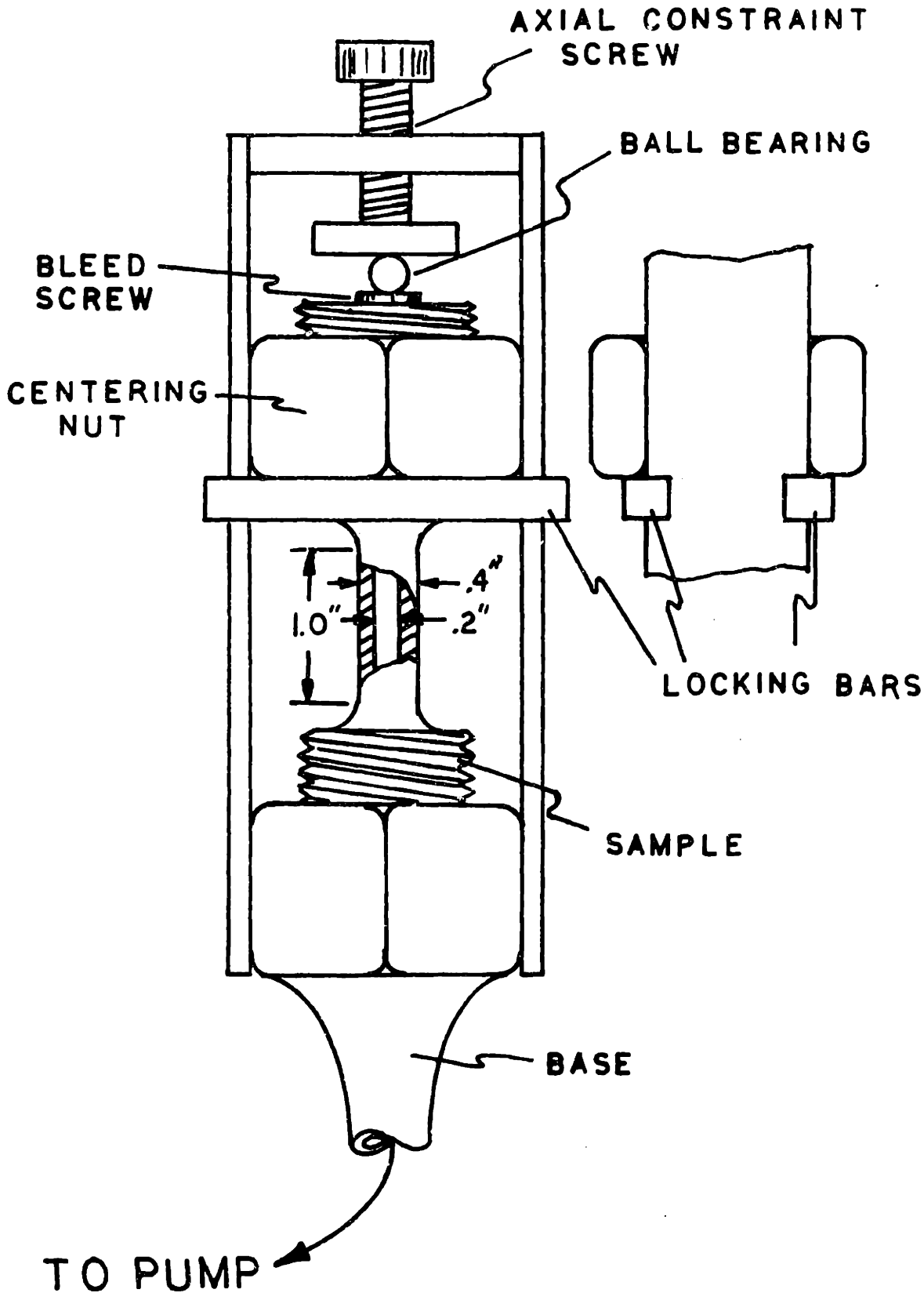

FIGURE 6.3.1 THICK WALLED CYLINDER SPECIMEN

6.4 RESULTS AND ANALYSIS

The results obtained from the experimentation are shown in as a plot of outside diameter vs. time in fig 6.4.1. Only the first 30 minutes of each test are included. Included in fig. 6.4.2 is a photograph of the specimen after the experiment at 700 psi. This fracture occured after 2 hours.

Using the data available from each of the tests performed, we performed a linear squares fit approximation to obtain the slope of each of the curves in fig. 6.4.1 . Each of these slopes corresponds to the outside diameter expansion rate, $\dot{D}$, at each pressure level. Then, the constant outside wall displacement rate, $\dot{U}_r(b)$, where **b** is the ouside radius, can be found using

$$\dot{U}_r(b) = \frac{\dot{D}}{2} \qquad 6.4.1$$

Having found the corresponding displacements rates, it is possible to find the corresponding radial strain rates at the outer surface of the cylinder

$$\dot{\epsilon}_{rr}(b) = - \frac{\dot{U}_r(b)}{b} \qquad 6.4.2$$

from the same set of equations, we can obtain the radial strain rate at the inside wall of the cylinder with

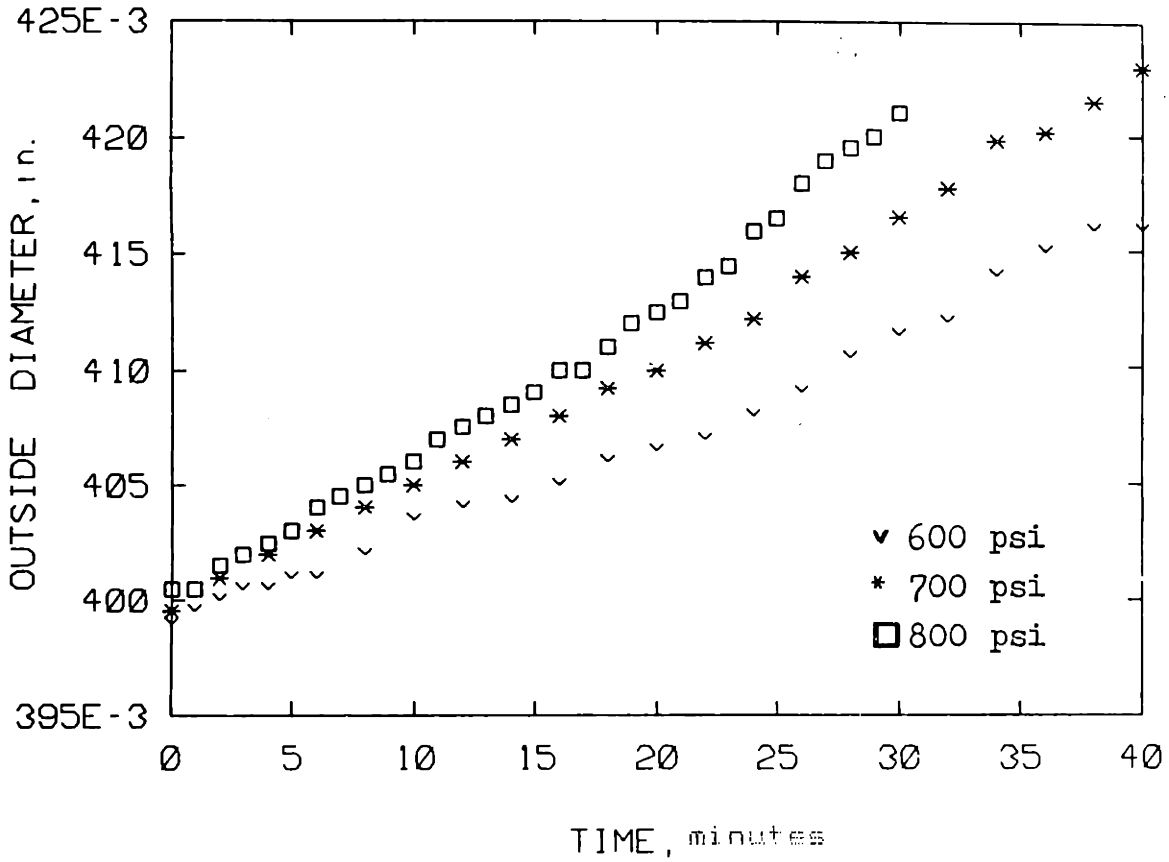

FIGURE 6.4.1 EXPERIMENTAL RESULTS OF A CREEPING THICK WALLED CYLINDER

FIGURE 6.4.2 VIEW OF THE THICK WALLED CYLINDER AFTER EXPERIMENTATION. PRESSURE=700 psi

$$\dot{\epsilon}_{rr}(a) = \frac{b^2}{a^2}\dot{\epsilon}_{rr}(b) \qquad 6.4.3$$

Using equation 6.4.3 and a log-log scale, we can plot the radial strain rate at the inner wall, $\dot{\epsilon}_{rr}(a)$, vs. the corresponding radial stress at the inner wall, σ_{rr}. We know that this stress is equal to

$$\sigma_{rr}(a) = -p$$

if we use the same assumptions presented in the Appendix D. plot of the three different data points corresponding to each pressure level can be seen in fig. 6.4.3 . Since the radial strain rate at the inner wall is a function of pressure

$$\dot{\epsilon}_{rr}(a) = f(p) \qquad 6.4.4$$

the three points in fig. 6.4.3 should form a straight line. The slope of this line corresponds to the material parameter **n**, which in this case was found to be **n**=1.914. With the value of **n**, it is then possible to find the value of **A** by using equation 6.2.1 and the equations that define equivalent strain rate and equivalent stress from the tensorial components. First, since the radial stress at the outer wall is

$$\sigma_{rr}(b) = 0$$

the equivalent stress at this location can be reduced to

$$\bar{\sigma}(b) = (3)^{\frac{1}{2}}\sigma_{zz}(b) \qquad 6.4.5$$

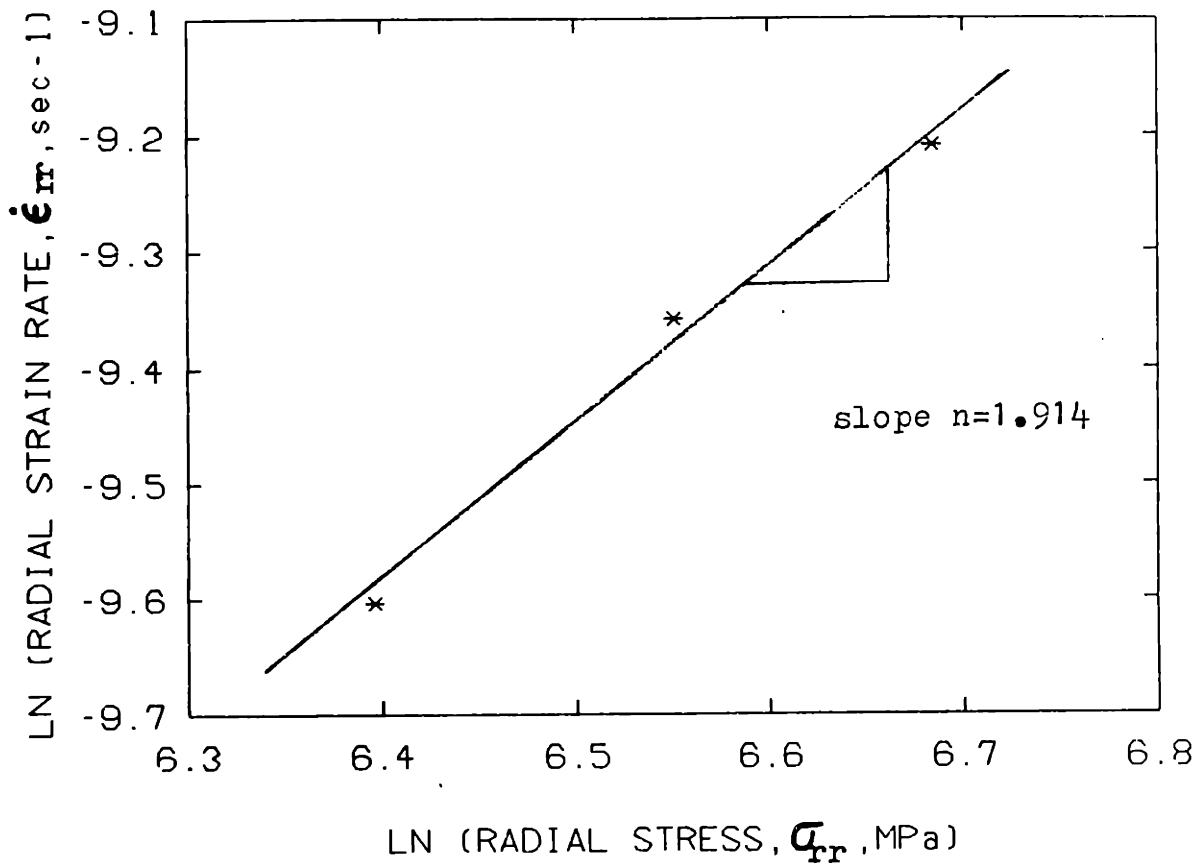

FIGURE 6.4.3 LOG-LOG PLOT OF STRESS VS. STRAIN RATE AT THE INNER WALL OF THE CYLINDER

Since the axial strain rate $\dot{\epsilon}_{zz}$ is zero, we can express the radial strain rate at the outside wall as

$$\dot{\bar{\epsilon}}^{c} = \frac{2}{(3)^{\frac{1}{2}}} \dot{\epsilon}_{rr}(b) \qquad 6.4.6$$

From the Appendix, the equation for $\sigma_{zz}(b)$ is

$$\sigma_{zz}(b) = \tfrac{1}{2}\left[\sigma_{rr}(b) + \sigma_{\theta\theta}(b)\right] \qquad 6.4.7$$

here, the values of $\sigma_{rr}(b)$ and $\sigma_{\theta\theta}(b)$ are taken from Appendix D. Substituting the above equations, 6.4.6, 6.4.7 and 6.4.8, into 6.4.1 we find that the value of **A** is

$$A = \frac{2}{[(3)^{\frac{1}{2}}]^{n+1}} \frac{\dot{\epsilon}_{rr}(b)}{(\sigma_{zz}(b))^{n}}$$

After introducing the corresponding values into eq.6.4.7, the value of **A** becomes $A=6.037\times10^{-5}$.

If we compare the values found in this section for the parameters **A** and **n**, with the values found by other researchers [20-23], we find that they are not in agreement. Since neither the material used in this experiment nor the actual experiment match exactly to the ones on the literature, these differences are expected.

In order to check the time integration procedure's ability to simulate actual experimental results, we performed a finite element simulation of this experiment. This was done by running a simple axisymmetric mesh to model the thick walled cylinder. Such a mesh was formed of 5 axisymmetric CAX8R type elements as shown in figure 6.4.4 .

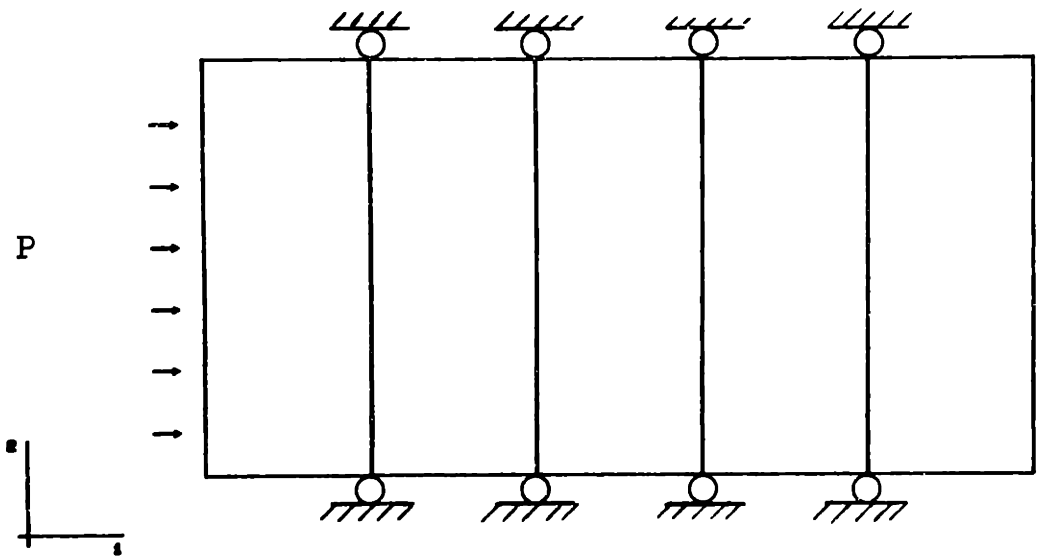

FIG 6.4.4 5 FINITE ELEMENT MESH OF THICK WALLED CYLINDER

The constitutive equations for this case, the power law model, was introduced into ABAQUS by means of a specially modified UMAT subroutine. This subroutine used the material properties found in [21] corresponding to a medium sized grain Solder. The values of **A** and **n** are the ones found from the experimental values.

After running the simulation based on the above outline, we ploted the results of the experiment and the ABAQUS results on fig. 6.4.5 . It can be appreciated how well the simulation results reproduce the experimental data.

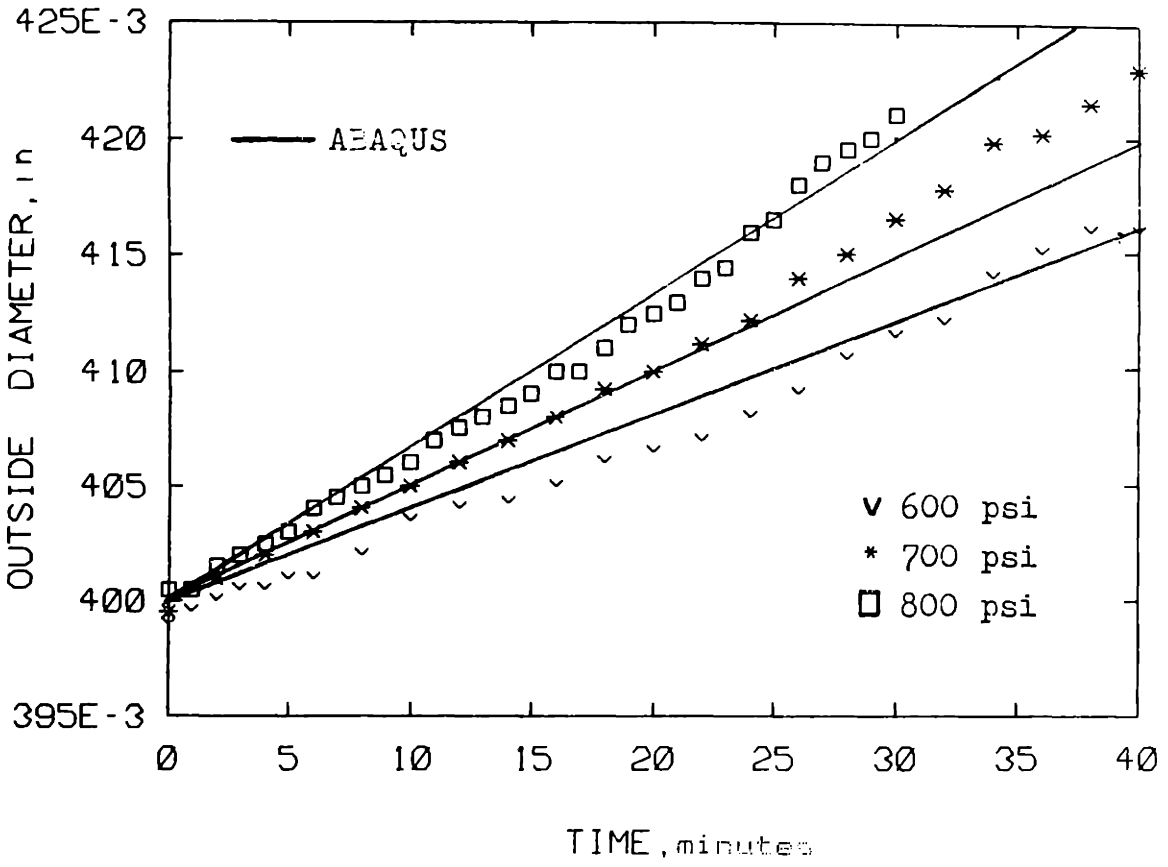

FIG 6.4.5 **EXPERIMENTAL AND ABAQUS RESULTS OF THE THICK WALL EXPERIMENT**

Chapter 7

CONCLUSIONS

Analytical simulations and experimental results showed that the time integration method proposed in this research can effectively reduce the amount of computer time required to solve problems related to rate dependent, high temperature deformations of metals, when compared to more classical models such as the Euler forward integration scheme. The use of θ=0.75 has been proven to yield unconditionally stable solutions, while introducing a small ammount of inaccuracy.

Using the automatic time step algorithm described in this research, the user can seclect a fixed tolerance (CETOL) which controls the accuracy of the integration results. This algorithm has been shown to reduce the nuber of time steps by 40%-60% when used to solve uniaxial probems while using no more than 2 interations per step in the areas of large stiffness.

The use of a user material subroutine UMAT introduced into the finite element code ABAQUS has been succefully used

to solve simple elasto-vicoplastic problems. By using UMAT we have succesfully extended the work of Pierce et al [1] to a complete finite element application using ABAQUS. Also, by introducing the effects of changing plastic flow, we have made the integration procedure compatible with more sophisticated problems

Results of a thick walled cylinder under internal pressure experiment has been succefully reproduced by using the time integration technique proposed in this research. Such findings prove the time integration abilities to solve real life problems.

Further numerical analysis needs still to be performed. The use of UMAT incorporated in ABAQUS should be used to solve more realistic finite elements models in oder to extend the validity of the integration method proposed. Examples of such models are the simulations of fully coupled temperature-deisplacement analysis, with the introduction of non adiabatic conditions.

REFERENCES

1. PEIRCE, D., SHIH, C. F., AND NEEDLEMAN, A. "A Tangent Modulus Method for Rate Dependent Solids", Computers and Structures, Vol. 18, 1984, pp. 875-890.

2. HIBBIT, KARLSSON, AND SORENSEN, "Abaqus User's Manual", Hibbit, Karlsson and Sorensen, Inc., 1984

3. BODNER, S.R., AND PARTOM, Y., "Constitutive Equations for Elasto-Viscoplastic Strain Hardening Materials", ASME Journal of Applied Mechanics, Vol. 42, 1975, pp.385-389

4. HART, E.W., "Cosntitutive Relations fot the Nonelastic Deformation of Metals", ASME Journal of Engineering Materials and Technology, Vol. 98, 1976, pp.97-113

5. ANAND, L., "Constitutive Equations for the Rate Dependent Deformation of Metals at Elevated Temperatures", ASME Journal of Engineering Materials and Technology, Vol. 104, 1982, pp. 12-17.

6. KRIEG, R.D., "Numerical Integration of Some New Unified Plasticity-Creep Formulations", Structural Mechanics in Reactor Technology, Vol. 4M, 1977, pp.M6/4

7. CYR , N. A., AND TETER,R. D., "Finite Element Elasto-Plastic-Creep Analysis of Two Dimensional Continuum with Teperature Dependent Material Properties", Computers and Structures, Vol. 3, 1973, pp.849-863

8. WILLAM, K.J., "Numerical Solution of Inelastic Rate Processes", Computers and Structures, Vol. 8, 1978, pp.511-531

9. SHIH, C.F., DELORENZI, H.G., AND MILLER, A.K., "A Stable Computational Scheme for Stiff Time-Dependent Constitutive Equations", SMIRT-4 Proc. Paper L 2/2, San Francisco, 1977

10. KANCHI, M. B., ZIENKIEWICZ, O. C., AND OWEN, D. R. J., " The Viscoplastic Approach to Problems of Plasticity and Creep Involving Geometric Non-Linear effects", International Journal for Numerical Methods in Engineering, Vol. 12, 1978, pp.169-181

11. ANAND, L., " Constitutive Equations for Hot Working", to appear in the International Journal of Plasticity.

12. LAMBERT, J.D., "Computational Methods in Ordinary Differential Equations", John Wiley and Sons, London, 1973

13. OWEN, D. R. J., AND HINTON, E., "Finite Elements in Plasticity: Theoty and Practice", Pineridge Press Limited, Swansea, U.K., 1980

14. SINCOVEC, R.F., "Numerical Methods for Differential Equations", University of Colorado, Release 1, Colorado Springs, 1981

15. ANAND, L., AND PARKS, D., Private communications., 1984

16. JOINT COMPUTER FACILITY, Penplot User Manual, Massachussetts Institute of Technology, 1981

17. GAROFALO, F., "Fundamentals of Creep and Creep Rupture in Metals", Mc Millan Co., New York, N.Y., 1965

18. ANAND, L., "A New Versatil High-Temperature Constitutive Model for ABAQUS" [Unpublished paper]

19. HIBBIT, KARLSSON AND SORENSEN, " ABAQUS Examples Problems", Hibbit, Karlsson and Sorensen, Inc., 1984

20. RHODE, R.W., AND SWEARENGEN, J.C.," Deformation Modeling Applied to Stress Relaxation of Four Solder Alloys", Journal of Engineering Materials and Technology, Vol. 102, 1980, pp.207-214

21. MOHAMED, F., AND LANGDON, T., "Creep Behavior in Superplastic Pb-62% Sn Eutectic", The Philosophical Magazine, Vol. 32, 1975, pp.697-709

22. BAKER, E., " Stress Relaxation in Tin-Lead Solders", Materials Science and Engineering, Vol. 38, 1979, pp.241-247

23. CAGNON, M., SUERY, M., EBERHARDT, A., AND BAUDELET, B., "High Temperature Deformation of The Pb-Sn Eutectic" Acta Metallurgica, Vol. 25, 1977, pp 71-75

APPENDIX A

```
C*************************************************************
C
C                Subroutine Umat
C
C     This subroutine introduces the integration scheme
C     into the ABAQUS codes. The Constitutive equations used are
C     the hot working equations developed by L. Anand. This
C     subroutine can be used with the *VISCO procedure, and
C     with the automatic time step control option
C
C*************************************************************
      SUBROUTINE UMAT(STRESS,STATEV,DDSDDE,SSE,SPD,
     1SCD,STRAN,DSTRAN,TIME,DTIME,TEMP,DTEMP,PREDEF,
     2DPRED,MATERL,NDI,NSHR,NTENS,NSTATV,PROPS,
     3NPROPS,COORDS)
C*************************************************************
      IMPLICIT REAL*8(A-H,O-Z)
C*************************************************************
      COMMON/CERROR/RESMAX(30),JNREMX(30),ERRMAX(2),CETOL,CSLIM,
     1 CEMAX,PCTOL,TLIMIT,PSUBIN,RESMIN,DUMAX(30),JNDUMX(30),
     2 ERRPRE,UDELSS,PTOL,AMTOL,DMKET,DMRETL,SIGTOL,DSIGMX,
     3 UTOL,UMAX,U4MAX,VMAX,V4MAX,AMAX,A4MAX,TMAX,EPPMAX,RMAX,R4MAX,
     4 NGOPEN,NGCLOS,ROTTOL,ROTFAC,JRIKND,NINCCS,RIKUB,RIKUMX,RIKMU,
     5 RIKLAM
     6,STRRAT,PCUT,RIKDLO
      DIMENSION STRESS(NTENS),STATEV(NSTATV),
     1DDSDDE(NTENS,NTENS),STRAN(NTENS),
     2DSTRAN(NTENS),PREDEF(1),DPRED(1),
     3PROPS(NPROPS),COORDS(3)
C*************************************************************
      DIMENSION DSTRES(6),STRESD(6)
C*************************************************************
C ELASTIC SHEAR AND BULK MODULI
C*************************************************************
      AMU=1.854E+3
      AKAPPA=4.017E+3
C*************************************************************
C COEFFICIENT OF THERMAL EXPANSION
C*************************************************************
      ALPHA=22.0E-6
C*************************************************************
C INITIAL VALUES OF STATE VARIABLES
C*************************************************************
      S0=51.81/1.7321
      T0=1223.0
      EDOT0=1.D-10
C*************************************************************
C THE PARAMETER PHI CONTROLS THE DEGREE OF IMPLICITNESS OF
C THE INTEGRATION PROCEDURE:
C PHI=0.0 ---- EXPLICIT
C PHI=1.0 ---- IMPLICIT
C*************************************************************
      PHI=0.75
C*************************************************************
C FOR ISOTHERMAL DEFORMATIONS SET OMEGA EQUAL TO ZERO.
C FOR ADIABATIC DEFORMATIONS THE PARAMETER OMEGA MUST BE
C SET TO A NON-ZERO VALUE OF APPROXIMATELY 0.9.
C RHO -----MASS DENSITY
C C   -----SPECIFIC HEAT
C*************************************************************
```

```
      OMEGA=0.9
      RHO=7.3
      C=0.669
C*****************************************************************
      DO 10 K1=1,NTENS
      DSTRES(K1)=0.0
10    CONTINUE
C*****************************************************************
      DO 20 K1=1,NTENS
      DO 20 K2=1,NTENS
      DDSDDE(K1,K2)=0.0
20    CONTINUE
C*****************************************************************
      CALL SINV(STRESS,SINV1,SINV2)
C*****************************************************************
      DO 30 K1=1,NDI
      STRESD(K1)=STRESS(K1)-SINV1
30    CONTINUE
C
      IF(NSHR.EQ.0) GO TO 50
C
      I1=NDI
      DO 40 K1=1,NSHR
      I1=I1+1
      STRESD(I1)=STRESS(I1)
40    CONTINUE
C
50    CONTINUE
C*****************************************************************
      S=STATEV(1)
      T=STATEV(2)
      EDOT1=STATEV(3)
C
      IF(STATEV(1).EQ.0.0)THEN
        S=S0
        T=T0
        EDOT1=EDOT0
        STATEV(1)=S0
        STATEV(2)=T0
        STATEV(3)=EDOT0
      END IF
C*****************************************************************
      TAUB=SINV2/1.73205081
      PB=-SINV1
C*****************************************************************
C THE NEXT CALL TO SBETA IS TO DETERMINE THE VALUE OF THE
C THE PLASTIC DILATANCY FACTOR BETA
C*****************************************************************
      CALL SBETA(TAUB,PB,T,S,BETA)
C*****************************************************************
C THE NEXT CALL TO GAMDOT IS TO DETERMINE THE EQUIVALENT
C PLASTIC SHEAR STRAIN RATE F AND THE PARTIAL DERIVATIVES
C PDA,PDB,PDC,PDD OF F WITH RESPECT TO TAUB,PB,T AND S,
C RESPECTIVELY.
C*****************************************************************
      CALL GAMDOT(TAUB,PB,T,S,F,PDA,PDB,PDC,PDD)
      STATEV(3)=F/1.73205081
      EDOT2=STATEV(3)
C*****************************************************************
C THE NEXT CALL TO SDOT IS TO DETERMINE THE HARDENING RATE H,
```

```
C THE STATIC RESTORATION RATE RDOT AND THE PARTIAL
C DERIVATIVES PDE AND PDF OF H AND RDOT, RESPECTIVELY, WITH
C RESPECT TO S.
C*****************************************************************
      CALL SDOT(TAUB,PB,T,S,F,H,RDOT,PDE,PDF)
C*****************************************************************
      PDG=PDE*F+PDD*H-PDF
      PDH=-PHI*DTIME*PDG
C
      HB=H/(1.+PDH)
      DR=RDOT*DTIME/(1.+PDH)
C
      G=AMU-(PDD*HB+PDB*AKAPPA*BETA
     1       +PDC*(OMEGA/(RHO*C))*(TAUB-BETA*PB))/PDA
C
      V=PHI*DTIME*PDA*G
C
      IF(PHI.EQ.0.0) THEN
        AMUB=AMU
        GO TO 55
      END IF
C
      H1=TAUB/(PHI*DTIME*F)
C
      AMUB=(AMU*H1)/(AMU+H1)
C
55    CONTINUE
C*****************************************************************
C THE NEXT BLOCK CALCULATES T'.DSTRAN
C*****************************************************************
      W1=0.0
      DO 60 K1=1,NDI
      W1=W1+STRESD(K1)*DSTRAN(K1)
60    CONTINUE
C
      IF(NSHR.EQ.0) GO TO 80
C
      I1=NDI
      DO 70 K1=1,NSHR
      I1=I1+1
      W1=W1+STRESD(I1)*DSTRAN(I1)
70    CONTINUE
C
80    CONTINUE
C*****************************************************************
C THE NEXT BLOCK CALCULATES TR(DSTRAN)
C*****************************************************************
      W2=0.0
      DO 90 K1=1,NDI
      W2=W2+DSTRAN(K1)
90    CONTINUE
C*****************************************************************
      V1=(F*DTIME)/(1.+V)
      V2=(V/(1.+V))*(1./G)
C*****************************************************************
C THE NEXT COMMAND CALCULATES THE EQUIVALENT PLASTIC SHEAR
C STRAIN INCREMENT.
C*****************************************************************
      DGAMPB=V1+V2*((AMU/TAUB)*W1+AKAPPA*(-PDB/PDA)*W2)
      STATEV(3)=EQUIVPS+DGAMPB
```

```
C**********************************************************************
C THE NEXT BLOCK CALCULATES THE INCREMENTS DS AND DT IN THE
C STATE VARIABLES S AND T, AND UPDATES THE VALUES OF THE
C STATE VARIABLES.
C**********************************************************************
      DS=HB*DGAMPB-DR
      DT=(OMEGA/(RHO*C))*(TAUB-BETA*PB)*DGAMPB
C
      STATEV(1)=S+DS
      STATEV(2)=T+DT
C**********************************************************************
C THE NEXT BLOCK CALCULATES THE STRESS INCREMENTS AND
C UPDATES THE VARIOUS COMPONENETS OF THE STRESS TENSOR.
C**********************************************************************
      V3=2.*AMUB
      V4=(AKAPPA-(2./3.)*AMUB)*W2
      V5=3.*AKAPPA*ALPHA*DT
      V6=AKAPPA*BETA*DGAMPB
      V7=V4-V5-V6
      V8A=(AMU/TAUB)*DGAMPB
      V8B=(AMU-AMUB)*W1/(TAUB**2.)
      V8=V8A-V8B
      V9=AMUB
C
      DO 100 K1=1,NDI
      DSTRES(K1)=V3*DSTRAN(K1)+V7-V8*STRESD(K1)
      STRESS(K1)=STRESS(K1)+DSTRES(K1)
100   CONTINUE
C
      IF(NSHR.EQ.0)GO TO 120
C
      I1=NDI
      DO 110 K1=1,NSHR
      I1=I1+1
      DSTRES(I1)=V9*DSTRAN(I1)-V8*STRESD(I1)
      STRESS(I1)=STRESS(I1)+DSTRES(I1)
110   CONTINUE
C
120   CONTINUE
C**********************************************************************
C THE NEXT BLOCK CALCULATES THE (IN GENERAL NON-SYMMETRIC)
C JACOBIAN MATRIX.
C**********************************************************************
      V10=AKAPPA
      V11=V10-(2./3.)*V9
      V12=(V2*(AMU/TAUB)**2.)-(AMU-AMUB)/(TAUB**2.)
      V13=V2*V10*(-PDB/PDA)*(AMU/TAUB)
      V14=V2*V10*BETA*(AMU/TAUB)
      V15=V2*(V10**2.)*BETA*(-PDB/PDA)
      V16=V11-V15
C
      DO 130 K1=1,NDI
      DDSDDE(K1,K1)=V3+V16
     1              -V12*STRESD(K1)**2.
     2              -(V13+V14)*STRESD(K1)
130   CONTINUE
C
      IF(NDI.EQ.1)GO TO 160
C
      DO 150 K1=2,NDI
```

```
      N2=K1-1
      DO 140 K2=1,N2
      DDSDDE(K2,K1)=V16-V12*STRESD(K2)*STRESD(K1)
     1             -V13*STRESD(K2)-V14*STRESD(K1)
      DDSDDE(K1,K2)=V16-V12*STRESD(K1)*STRESD(K2)
     1             -V13*STRESD(K1)-V14*STRESD(K2)
140   CONTINUE
150   CONTINUE
160   CONTINUE
C
      IF(NSHR.EQ.0)GO TO 200
C
      DO 180 K1=1,NDI
      I1=NDI
      DO 170 K2=1,NSHR
      I1=I1+1
      DDSDDE(K1,I1)=-V12*STRESD(K1)*STRESD(I1)
     1             -V14*STRESD(I1)
      DDSDDE(I1,K1)=-V12*STRESD(I1)*STRESD(K1)
     1             -V13*STRESD(I1)
170   CONTINUE
180   CONTINUE
C
      I1=NDI
      DO 190 K1=1,NSHR
      I1=I1+1
      DDSDDE(I1,I1)=V9-V12*STRESD(I1)*STRESD(I1)
190   CONTINUE
C
      IF(NSHR.EQ.1) GO TO 200
C
      IF(NSHR.EQ.2) THEN
        I=NDI+1
        J=NDI+2
        DDSDDE(I,J)=-V12*STRESD(I)*STRESD(J)
        DDSDDE(J,I)=DDSDDE(I,J)
      END IF
C
      IF(NSHR.EQ.3) THEN
        I=NDI+1
        J=NDI+2
        K=NDI+3
        DDSDDE(I,J)=-V12*STRESD(I)*STRESD(J)
        DDSDDE(J,I)=DDSDDE(I,J)
        DDSDDE(I,K)=-V12*STRESD(I)*STRESD(K)
        DDSDDE(K,I)=DDSDDE(I,K)
        DDSDDE(J,K)=-V12*STRESD(J)*STRESD(K)
        DDSDDE(K,J)=DDSDDE(J,K)
      END IF
C
200   CONTINUE
C
C*****************************************************************
C CALCULATION OF THE PLASTIC STRAIN RATES BEFORE AND AFTER
C THE TIME STEP,TO BE USED BY THE AUTOMATIC INTEGRATION
C SCHEME OF ABAQUS
C*****************************************************************
      DIFF=DTIME*DABS(DABS(EDOT1)-DABS(EDOT2))
      CEMAX=DMAX1(CEMAX,DIFF)
      RETURN
```

```
      END
C*****************************************************************
C
C*****************************************************************
      SUBROUTINE SBETA(TAUB,PB,T,S,BETA)
C*****************************************************************
      IMPLICIT REAL*8(A-H,O-Z)
C*****************************************************************
      BETA=0.0
C
      RETURN
      END
C*****************************************************************
C
C*****************************************************************
      SUBROUTINE GAMDOT(TAUB,PB,T,S,F,PDA,PDB,PDC,PDD)
C*****************************************************************
      IMPLICIT REAL*8(A-H,O-Z)
C*****************************************************************
C MATERIAL PARAMETERS DEFINING THE FUNCTION F  FOR THE
C EQUIVALENT PLASTIC SHEAR STRAIN RATE:
C A ----PRE-EXPONENTIAL FACTOR
C Q ----ACTIVATION ENERGY
C R ----UNIVERSAL GAS CONSTANT
C AM ---STRAIN RATE SENSITIVITY
C PALPHA ---PRESSURE SENSITIVITY PARAMETER
C PALPHA=2*(DMU/DPB)/MUO
C MUO ---SHEAR MODULUS AT ZERO PRESSURE
C DMU/DBP -----PRESSURE DEPENDENCY OF SHEAR MODULUS
C*****************************************************************
      A=1.7321E+11
      Q=270.0
      R=8.31E-3
      AM=0.147
      PALPHA=0.0
C*****************************************************************
      IF(TAUB.LT.0.001) THEN
        TAUB=.001
      END IF
C
      A1=A*DEXP(-Q/(R*T))
C
      F=A1*(TAUB/(S*(1.+PALPHA*PB)))**(1./AM)
C
      IF(F.LT.1.D-10)THEN
        F=1.D-10
      END IF
C
      PDA=F/(AM*TAUB)
      PDB=-(S*PALPHA)*F/(AM*(S*(1.+PB*PALPHA)))
      PDC=F*(Q/(R*T**2.))
      PDD=-F/(AM*S)
C
      RETURN
      END
C*****************************************************************
C
C*****************************************************************
      SUBROUTINE SDOT(TAUB,PB,T,S,F,H,RDOT,PDS,PDF)
C*****************************************************************
```

```
      IMPLICIT REAL*8(A-H,O-Z)
C*****************************************************************
C MATERIAL PARAMETERS DETERMINING THE RATE OF HARDENING:
C HO -------MAXIMAL HARDENING RATE
C SB -------PRE-MULTIPLIER FOR SATURATION VALUE OF S
C A --------PRE- EXPONENTIAL FACTOR IN F
C Q  -------ACTIVATION ENERGY
C R --------UNIVERSAL GAS CONSTANT
C AN -------EXPONENT IN EQN. FOR SATURATION VALUE OF S
C AMU ------SHEAR MODULUS
C SA -------ANNEALED VALUE OF S. A FUNCTION OF TEMP.
C B --------PRE-MULTIPLIER FOR RATE OF STATIC RESTORATION
C P --------EXPONENT OF ((S/SA)-1.) IN RDOT
C*****************************************************************
      HO=1329.22/3.
      SB=147.6/1.7321
      A=1.7321E+11
      Q=270.0
      R=8.31E-3
      AN=0.03
      AMU=1.854E+3
      SA=50.59/1.7321
      B=0.0
      P=3.5
C*****************************************************************
      IF(F.LT.1.0D-10) THEN
        F=1.0D-10
      END IF
C*****************************************************************
      A1=A*DEXP(-Q/(R*T))
C
      SS=SB*(F/A1)**AN
C
C
      H=HO*(1.-S/SS)
      PDE=-HO/SS
      B1=B*A1
C
      RDOT=0.0
      PDF=0.0
      SD=(S/SA)-1.
C
      IF(SD.LT.0.0)THEN
      S=SA
      END IF
C
      IF(SD.GT.0.0)THEN
      RDOT=AMU*B1*SD**P
      PDF=AMU*B1*(P/SA)*SD**(P-1.)
      END IF
C
      RETURN
      END
```

```
C
C*****************************************************************************
C
C                                  HITREHD
C                                  -------
C
C
C       The subroutine HITREHD will compute the solutions for stress,strain
C      and the internal variable "s" or hardness of a given material, using
C      a ramp strain rate test. The equations used are the constitutive eq.'s
C      for the description of high temperature, large rate-dependant defor-
C      tions using static recovery functions and internal heat generation.
C      The integration procedure used is the called rate tangent modulus
C      method in its implicit form only(phi>0.5), implemented with the usage
C      of an automatic time step control in order to minimize total #of steps
C
C
C*****************************************************************************
C
C    The imput required for this program is:
C
C                              MATERIAL PARAMETERS
C                              -------------------
C
C    TEMP= Initial temperature                 A= material parameter
C    EDT1= initial strain rate                 Q= Activation energy
C    ELM= Initial strain limit                 XM= strain energy sensitivity
C    E= incremental Young's modulus            Ho= initial strain hardening rate
C    So= initial internal variable S           Sb= internal parameter
C    N= matrial parameter                      B= recovery function parameter
C    p= recovery function exponent             xnu=poisson ratio
C    w= % of energy transformed into heat      ro=density
C    spheat= specific heat
C
C
C                              INTEGRATION PARAMETERS
C                              ----------------------
C
C    psi= rate tangent modulus parameter       dtmax=#times*(minimun time step)
C    CALPHA= integration sensitivity           icurv= #of periods to be ploted
C
C
C*****************************************************************************
C
C
      COMMON STRESS(1500),STRAIN(1500),SIV(1500),STEP(1500),TEMP(1500),
     #E(1500),XNU(1500),ALPHA(1500),BETA(1500),RO(1500),SPHEAT(1500)
      READ(5,*)ICURV
      DO 110 KT=1,ICURV
      READ(5,*)TEMPO,EDT1,ELM,ELM2,EO,A,Q,XM,XN
      READ(5,*)HO,SO,SB,PSI,B,P,CALPHA,DTMAX,IXM
      READ(5,*)W,ALPHAO,XNUO,ROO,SPHEATO
      WRITE(6,*)TEMPO,EDT1,ELM,ELM2,EO,A,Q,XM,XN,HO,SO,SB
      WRITE(6,*)PSI,B,P,W,ALPHAO,XNUO,ROO,SPHEATO
C
C  The flags klin and klon work as stress and strain delimeting parameters
C
      NI=2
      KLIN=0
      KLON=0
C
```

```
C  defining test constants
C
      R=8.31E-03
      CETOL=CALPHA*SO/EO
      C=A*EXP(-Q/(R*TEMPO))
C
C  Defining the initial conditions
C
      EDT=EDT1
      DTM=.01*(SO/(EO*ABS(EDT)))
      DTMAX=DTMAX*(DTM)
      SSTP=0.
      SSTPP=0.
      STRESS(1)=0.0001
      STRAIN(1)=0.
      SIV(1)=SO
      TEMP(1)=TEMPO
      E(1)=EO
      ALPHA(1)=ALPHAO
      XNU(1)=XNUO
      RO(1)=ROO
      SPHEAT(1)=SPHEATO
      BETA(1)=E(1)*ALPHA(1)/(1.-2*XNU(1))
C
C  The ffollowing procedure uses the constitutive eq.'s to compute the desired
C  values
C
      KLAN=0
      KLUN=0
      IO=0
      DO 30 II=NI,1500
      I=IO+II
      WRITE(6,*)I
      C=A*EXP(-Q/(R*TEMP(I-1)))
      SFN=C*(ABS(STRESS(I-1))/SIV(I-1))**(1./XM)
      IF(SFN.LT.1.E-28)SFN=1.E-28
      ST=SB*(ABS(EDT)/C)**XN
      HSN=HO*(1.-SIV(I-1)/ST)
      XRCO=(SIV(I-1)/SO)-1.
      IF(XRCO.GT.0.)THEN
         RCO=(C/A)*B*E(I-1)*(XRCO)**P
         ELSE
         XRCO=0.0001
         RCO=0.0001
      END IF
      D=SFN/(XM*ABS(STRESS(I-1)))
      G=-Q*SFN/(R*(TEMP(I-1))**2)
      XI=-SFN/(XM*SIV(I-1))
      XK=RCO*P/(SO*XRCO)
      XC=-HO/ST
      XNN=XC*SFN+XI*HSN-XK
      XP=-PSI*DTM*XNN
      HN=HSN/(1.+XP)
      DRCO=RCO*DTM/(1.+XP)
      T=E(I-1)-XI*HN/D+(SIGN(BETA(I-1),STRESS(I-1))-G/D)
     #*W*ABS(STRESS(I-1))/(RO(I-1)*SPHEAT(I-1))
      U=PSI*DTM*D*T
      F=SFN/(1.+U)
      DSTR=EDT*DTM
      DSTRP=DTM*SIGN(F,STRESS(I-1))+PSI*DTM*D
```

```
     #*E(I-1)*DSTR/(1.+U)
        DSTRPS=DTM*SIGN(F,STRESS(I-1))+PSI*DTM*D
     #*E(I-1)*ABS(DSTR)/(1.+U)
        DTEMP=W*ABS(STRESS(I-1))*ABS(DSTRP)/(RO(I-1)*SPHEAT(I-1))
        DSTRESS=E(I-1)*(DSTR-DSTRP)-BETA(I-1)*DTEMP
        DSIV=ABS(HN*DSTRPS)-DRCO
C
C  The following loop performs the automatic control of the time step
C
        DO 10 J=1,500
        STRAIN(I)=STRAIN(I-1)+DSTR
        STRESS(I)=STRESS(I-1)+DSTRESS
        SIV(I)=SIV(I-1)+DSIV
        STEP(I)=DTM
        TEMP(I)=TEMP(I-1)+DTEMP
        E(I)=E(I-1)
        XNU(I)=XNU(I-1)
        ALPHA(I)=ALPHA(I-1)
        BETA(I)=BETA(I-1)
        RO(I)=RO(I-1)
        SPHEAT(I)=SPHEAT(I-1)
        C=A*EXP(-Q/(R*TEMP(I)))
        ST=SB*(ABS(EDT)/C)**XN
        XEPDTN=C*((ABS(STRESS(I))/SIV(I))**(1./XM))
        EPDTN=SIGN(XEPDTN,STRESS(I))
        XMDPSI1=DTM*ABS(ABS(EPDTN)-ABS(SFN))
        XRCO=(SIV(I)/SO)-1.
        IF(XRCO.GT.0.)THEN
           RCO=(C/A)*B*E(I)*(XRCO)**P
           ELSE
           RCO=0.
        END IF
        SDOTN=HO*(1.-SIV(I)/ST)*ABS(EPDTN)-RCO
        XMDPSI2=DTM*ABS(SDOTN-DSIV/DTM)/E(I)
        IF(XMDPSI1.GE.XMDPSI2)THEN
           XMDPSI=XMDPSI1
           ELSE
           XMDPSI=XMDPSI2
        END IF
        IF(IXM.EQ.0)XMDPSI=XMDPSI1
        RI=XMDPSI/CETOL
        IF(DTM.LT.STEP(2)) THEN
          DTM=STEP(2)
          GOTO 10
          ELSE
          END IF
        IF(DTM.EQ.STEP(2))GO TO 20
        IF(RI.LE.1.0)GO TO 20
        DTM=(0.85/RI)*DTM
   10   CONTINUE
C
C  the following procedure controls the data according to the ramp test
C

   20   IF(STRAIN(I).GE.ELM2)GO TO 50
C
C  The following if blocks control the value of the next time step to
C  be used in the integration point corresponding to I+1
C
        IF(0.7.LT.RI.LE.0.8)DTM=1.1*DTM
```

```
      IF(0.4.LT.RI.LE.0.7)DTM=1.25*DTM
      IF(RI.LE.0.4)DTM=1.5*DTM
      IF(DTM.GE.DTMAX)DTM=DTMAX
30    CONTINUE
C
C  The output of the program
C
50    INT=I-1
      WRITE(6,60)INT,PSI
60    FORMAT(/,/,8X,'NUMBER OF STEPS COMPUTED= ',I8,/,8X,'PSI USED=',
     #F4.2)
      WRITE(6,70)
70    FORMAT(/,/,10X,90('*'),/)
      WRITE(6,80)
80    FORMAT(14X,'STRESS',6X,'STRAIN',9X,'S',8X,'STEP',5X,'TEMP')
      WRITE(6,90)
90    FORMAT(/,10X,90('*'),/)
      WRITE(6,100)(STRESS(K),STRAIN(K),SIV(K),STEP(K),TEMP(K),K=1,I)
100   FORMAT(12X,5E12.5)
      CALL PLOTIN(I,KT,ICURV)
110   CONTINUE
      STOP
      END
C
C  The following subroutine plots the Stress VS. strain
C
      SUBROUTINE PLOTIN(IC,LI,MFIN)
      COMMON STRESS(1500),STRAIN(1500)
      REAL GRAP(2,1500),XL(4)
      DATA XL,LQM/0.,0.18,0.,60.,01/
      DO 10 KP=1,IC
      GRAP(1,KP)=STRESS(KP)
      GRAP(2,KP)=STRAIN(KP)
10    CONTINUE
      IF(LI.GT.1)LQM=11
      IF(LI.EQ.MFIN)LQM=10
      CALL QPICTR(GRAP,2,IC,QX(2),QMOVE(LQM),QLABEL(13),
     #QISCL(-2),QXSCL(XL))
      RETURN
      END

C
C  The function xintplt will interpolate to find an unknown value of X3,
C  where X1<X3<X2.
C
      FUNCTION XINTPLT(X1,X2,Y1,Y2,Y3)
      XINTPLT=((X2-X1)*(Y3-Y1)/(Y2-Y1))+X1
      RETURN
      END
C
C  the function extplt will extrapolate to find an unknown value of Y3,
C  which lies between Y1 and Y2, where Y1<Y3<Y2
C
      FUNCTION EXTPLT(X1,X2,X3,Y1,Y2)
      EXTPLT=((X3-X1)*(Y2-Y1)/(X2-X1))+Y1
      RETURN
      END
```

APPENDIX B

We now present the derivation of the material equations increments presented in Section 5.2. These calculations form part of the UMAT subroutine, and were derived for Anand [31].

If we define the increment of the equivalent plastic shear strain increment

$$\Delta\bar{\gamma}^p(n) = \Delta t(n)\ [f(n) + \phi\ \{f(n+1) - f(n)\}]$$

where

$$\dot{\bar{\gamma}}^p = f(n)$$

Let

$$PDA(n) = \partial f(n)/\partial\bar{\tau}(n)$$

$$PDC(n) = \partial f(n)/\partial\theta(n)$$

$$PDD(n) = \partial f(n)/\partial S(n)$$

then

$$f(n+1) - f(n) \doteq PDA(n)\ \Delta\bar{\tau}(n) + PDC(n)\ \Delta\theta(n) + PDD(n)\ \Delta S(n)$$

We now successively estimate $\Delta\bar{\tau}$, $\Delta\theta$, and ΔS:

1) $\underline{\Delta\bar{\tau}}$

$$\dot{\bar{\tau}} = [\{(1/2)\ \underline{\sigma}'.\ \underline{\sigma}'\}^{1/2}]^{\cdot} = \left(\frac{\underline{\sigma}'}{2\bar{\tau}}\right).\ \dot{\underline{\sigma}}$$

$$\dot{\bar{\tau}} = \left(\frac{\sigma'}{2\bar{\tau}}\right) \cdot \underline{L} \left[\dot{\underline{\varepsilon}} - \dot{\underline{\varepsilon}}^p\right]$$

Let

$$\underline{N} = \left(\frac{\sigma'}{2\bar{\tau}}\right)$$

then

$$\dot{\underline{\varepsilon}}^p = \dot{\gamma}^p \left[\underline{N}\right]$$

$$\dot{\bar{\tau}} = \underline{N} \cdot \underline{L} \left[\dot{\underline{\varepsilon}}\right] - \underline{N} \cdot \underline{L} \left[\underline{N}\right] \dot{\gamma}^p$$

$$\dot{\bar{\tau}} = \underline{L} \left[\underline{N}\right] \cdot \dot{\underline{\varepsilon}} - \underline{N} \cdot \underline{L} \left[\underline{N}\right] \dot{\gamma}^p$$

$$\underline{L} \left[\underline{N}\right] = 2\mu \left(\frac{\sigma'}{2\bar{\tau}}\right) = \left(\frac{\mu}{\bar{\tau}}\right) \underline{\sigma}'$$

$$\underline{N} \cdot \underline{L} \left[\underline{N}\right] = \left(\frac{\sigma'}{2\bar{\tau}}\right) \cdot \left(\frac{\mu}{\bar{\tau}}\right) \underline{\sigma}' = \mu \frac{\sigma' \cdot \sigma'}{2\bar{\tau}^2} = \mu$$

$$\dot{\bar{\tau}} = \left(\frac{\mu}{\bar{\tau}}\right) \underline{\sigma}' \cdot \dot{\underline{\varepsilon}} - \mu \dot{\gamma}^p$$

$$\Delta\bar{\tau} = \left(\frac{\mu}{\bar{\tau}}\right) \underline{\sigma}' \cdot \Delta\underline{\varepsilon} - \mu \Delta\bar{\gamma}^p$$

2) $\underline{\Delta\theta}$

$$\dot{\theta} = \left(\frac{\omega}{\rho c}\right) \underline{\sigma} \cdot \dot{\underline{\varepsilon}}^p$$

$$= \left(\frac{\omega}{\rho c}\right) \left\{\underline{\sigma} \cdot \left[\left(\frac{\sigma'}{2\bar{\tau}}\right)\right]\right\} \dot{\gamma}^p$$

$$\dot{\theta} = \frac{\omega}{\rho c} \left\{\bar{\tau}\right\} \dot{\gamma}^p$$

$$\Delta\theta = (\omega/\rho c)\ (\bar{\tau})\ \Delta\bar{\gamma}^{p}$$

3) $\underline{\Delta S}$

$$\Delta S(n) = \Delta t(n)\ [\dot{S}(n) + \phi\ \{\dot{S}(n+1) - \dot{S}(n)\}]$$

Let

$$PD1 = \frac{\partial h}{\partial \bar{\tau}} \qquad PD3 = \frac{\partial h}{\partial \theta} \qquad PDE = \frac{\partial h}{\partial S} \qquad PD4 = \frac{\partial \dot{\Gamma}}{\partial \theta}$$

$$PDF = \frac{\partial \dot{\Gamma}}{\partial S}$$

then

$$\dot{S}(n+1) \doteq [h(n) + PD1\ \Delta\bar{\tau}(n) + PD3\ \Delta\theta(n) + PDE\ \Delta S(n)]\ x$$

$$[f(n) + PDA\ \Delta\bar{\tau}(n) + PDC\ \Delta\theta(n) + PDD\ \Delta S(n)]$$

$$- [\dot{\Gamma}(n) + PD4\ \Delta\theta(n) + PDF\ \Delta S(n)]$$

Let

$$PD5 = PD1\ x\ f + PDA\ x\ h$$

$$PD7 = PD3\ x\ f + PDC\ x\ h - PD4$$

$$PDG = PDE\ x\ f + PDD\ x\ h - PDF$$

Then to first order in increments

$$\dot{S}(n+1) - \dot{S}(n) \doteq PD5 \times \Delta\tau(n) + PD7 \times \Delta\theta(n) + PDG \times \Delta S(n)$$

$$\Delta S(n) = \dot{S}(n)\,\Delta t(n) + \phi\,\Delta t(n)\,PDG \times \Delta S(n) + 0\,(\Delta t(n)^2)$$

Let

$$PDH = -\phi\,\Delta t\,PDG$$

then

$$\Delta S(n) = \frac{\dot{S}(n)\,\Delta t(n)}{(1 + PDH)}$$

Let

$$HB = \frac{h}{1 + PDH}$$

$$\Delta R = \frac{\dot{\Gamma}\,\Delta t}{(1 + PDH)}$$

then

$$\Delta S = HB \times \Delta\bar{\gamma}^p - \Delta R$$

Finally

$$\Delta\bar{\gamma}^p = f \times \Delta t + \phi\,\Delta t\,[PDA\,\{(\frac{\mu}{\bar{\tau}})\,(\sigma' \cdot \Delta\varepsilon) - \mu\,\Delta\bar{\gamma}^p\} + PDC\,\{(\frac{\omega}{\rho C})(\bar{\tau} - \Delta\bar{\gamma}^p\} + PDD\,\{HB \times \Delta\bar{\gamma}^p - \Delta R\}]$$

$$\Delta\bar{\gamma}^p = f \times \Delta t + \phi\, \Delta t\, PDA \left[\left(\frac{\mu}{\bar{\tau}}\right) \left(\underline{\sigma}' \cdot \Delta\underline{\varepsilon}\right) \right.$$

$$- \left[\phi\, \Delta t\, PDA \left[\mu - \frac{PDC}{PDA} \left(\frac{\omega}{\rho C}\right)(\bar{\tau}) \right.\right.$$

$$\left.\left. - \frac{PDD}{PDA} HB \right] \right] \Delta\bar{\gamma}^p$$

$$- \phi\, \Delta t\, PDD\, \Delta R$$

Let

$$G = \mu - \{ PDC \left(\frac{\omega}{\rho C}\right) (\bar{\tau}) + PDD\, HB \} / PDA$$

$$V = \phi\, \Delta t\, PDA\, G$$

then

$$\phi\, \Delta t\, PDA = \frac{V}{G}$$

and

$$(1 + V)\, \Delta\bar{\gamma}^p = f \times \Delta t + \frac{V}{G} \left[\left(\frac{\mu}{\bar{\tau}}\right) \left(\underline{\sigma}' \cdot \Delta\underline{\varepsilon}\right) \right]$$

$$- \phi\, \Delta t\, PDD\, \Delta R$$

$$\Delta\bar{\gamma}^p = \left(\frac{f\, \Delta t}{1 + V}\right) + \left(\frac{V}{1 + V}\right)\left(\frac{1}{G}\right) \left[\left(\frac{\mu}{\bar{\tau}}\right) \left(\underline{\sigma}' \cdot \Delta\underline{\varepsilon}\right) \right.$$

$$\Delta\bar{\gamma}^p = \left\{ \left(\frac{f}{1 + V}\right) \Delta t \right\} + \left(\frac{V}{1 + V}\right) \left(\frac{1}{G}\right) \left[\underline{M} \cdot \Delta\underline{\varepsilon} \right]$$

where

$$\underline{M} = \left[\left(\frac{\mu}{\bar{\tau}}\right) \sigma' \right]$$

APPENDIX C

```
*HEADING
UNIAXIAL TESION TEST USING UMAT
*NODE
1,0.0,0.0
2,0.5,0.0
3,0.5,1.0
4,0.0,1.0
*NSET,NSET=EDGET
3,4
*ELEMENT,TYPE=CAX4H
1,1,2,3,4
*BOUNDARY
1,1,2
2,2
4,1
*EQUATION
2
3,1,1.,2,1,-1.
*MATERIAL
*USER MATERIAL,CONSTANTS=1
1.
*DEPVAR
3
*STEP,INC=150,CYCLE=10,NLGEOM,AMP=RAMP
*VISCO,PTOL=5.0E-5,CETOL=8.0E-4
0.025,6.52,0.005,0.4
*BOUNDARY
EDGET,2,,0.15
*EL PRINT,FREQUENCY=10
2,1
2,1,1
*NODE PRINT,FREQUENCY=100
*EL FILE,FREQUENCY=1
2,1
2,1,1
*END STEP
```

```
*HEADING
THICK WALL TUBE, UMAT2
*NODE
1,0.1,0.
11,0.2,0.
51,0.1,0.05
61,0.2,0.05
101,0.1,0.1
111,0.2,0.1
*NGEN,NSET=SIDE1
1,11,1
*NGEN,NSET=SIDE3
101,111,1
*NGEN,NSET=SIDE2
51,61,1
*NSET,NSET=IN
1,51,101
*NSET,NSET=OUT
11,61,111
*NSET,NSET=SIDES
SIDE1,SIDE3
*ELEMENT,TYPE=CAX8R
1,1,3,103,101,2,53,102,51
*ELGEN
1,5,2,1
*MATERIAL
*USER MATERIAL,CONSTANTS=1
1.
*DEPVAR
2
*BOUNDARY
SIDES,2
*STEP,INC=1,CYCLE=10
*STATIC,PTOL=1.,DIRECT
0.02,0.02
*DLOAD
1,P4,0.7
*EL PRINT,COORDS
2,1
2,1,1
*NODE PRINT
*NODE FILE,NSET=OUT
2,1
*END STEP
*STEP,INC=101,CYCLE=10
*STATIC,PTOL=10.,DIRECT
0.02,2.
*EL PRINT,COORDS,FREQ=50
2,1
2,1,1
*NODE PRINT,FREQ=50
*NODE FILE,NSET=OUT,FREQ=20
2,1
*END STEP
*STEP,INC=135,CYCLE=10,AMP=STEP,NLGEOM
*VISCO,PTOL=1.,CETOL=1.E-4
55.,7200.
*EL PRINT,COORDS,FREQ=50
2,1
2,1,1
*NODE PRINT,FREQ=50
*NODE FILE,FREQ=2,NSET=OUT
2,1
*END STEP
```

```
*HEADING
THICK WALL TUBE, UMAT2
*NODE
1,0.1,0.
11,0.2,0.
51,0.1,0.05
61,0.2,0.05
101,0.1,0.1
111,0.2,0.1
*NGEN,NSET=SIDE1
1,11,1
*NGEN,NSET=SIDE3
101,111,1
*NGEN,NSET=SIDE2
51,61,1
*NSET,NSET=IN
1,51,101
*NSET,NSET=OUT
11,61,111
*NSET,NSET=SIDES
SIDE1,SIDE3
*ELEMENT,TYPE=CAX8R
1,1,3,103,101,2,53,102,51
*ELGEN
1,5,2,1
*MATERIAL
*USER MATERIAL,CONSTANTS=1
1.
*DEPVAR
2
*BOUNDARY
SIDES,2
*STEP,INC=1,CYCLE=10
*STATIC,PTOL=1.,DIRECT
0.02,0.02
*DLOAD
1,P4,0.7
*EL PRINT,COORDS
2,1
2,1,1
*NODE PRINT
*NODE FILE,NSET=OUT
2,1
*END STEP
*STEP,INC=101,CYCLE=10
*STATIC,PTOL=10.,DIRECT
0.02,2.
*EL PRINT,COORDS,FREQ=50
2,1
2,1,1
*NODE PRINT,FREQ=50
*NODE FILE,NSET=OUT,FREQ=20
2,1
*END STEP
*STEP,INC=135,CYCLE=10,AMP=STEP,NLGEOM
*VISCO,PTOL=1.,CETOL=1.E-4
55.,7200.
*EL PRINT,COORDS,FREQ=50
2,1
2,1,1
```

APPENDIX D

Given the power law form of eq. 6.2.1, we can make the following assumptions in order to find a analytical solution for the thick walled cylinder: (a) the material is incompressible, (b) the cylinder expands in an axisymmetrical fashion, (c) the condition of plane strain prevails, and (d) the stresses remain steady so that elastic strain rates will vanish.

Then the solution for a creeping cylinder, of inside radius **a** and outside radius **b**, under internal pressure **p** is:

$$\dot{\epsilon}_{\theta\theta}(r) = A\left(\tfrac{3}{4}\right)^{(n+1)/2}\left[\frac{2p}{(b/a)^{2/n}-1}\,\frac{1}{n}\right](b/r)^2$$

$$\sigma_{rr}(r) = -p\,\frac{(b/r)^{2/n}-1}{(b/a)^{2/n}-1}$$

$$\sigma_{\theta\theta}(r) = p\,\frac{[2-n]/n]\,(b/r)^{2/n}+1}{(b/a)^{2/n}-1}$$

$$\sigma_{zz}(r) = \tfrac{1}{2}\left[\sigma_{\theta\theta}+\sigma_{rr}\right]$$